

APPENDIX 2.10.2

TABLE OF CONTENTS

	<u>Page</u>
2.10.2 NUHOMS®-MP197 CASK LID BOLT ANALYSIS	2.10.2-1
2.10.2.1 Introduction.....	2.10.2-1
2.10.2.2 Lid Bolt Calculations.....	2.10.2-2
2.10.2.3 Load Combinations.....	2.10.2-9
2.10.2.4 Bolt Stress Calculations	2.10.2-12
2.10.2.5 Analysis Results	2.10.2-14
2.10.2.6 Fatigue Analysis.....	2.10.2-15
2.10.2.7 Minimum Engagement Length for Bolt and Flange.....	2.10.2-20
2.10.2.8 Ram Port Cover Bolt Analysis.....	2.10.2-22
2.10.2.9 Conclusions.....	2.10.2-33
2.10.2-10 References.....	2.10.2-34

LIST OF TABLES

2.10.2-1	Design Parameters for Lid Bolt Analysis
2.10.2-2	Bolt Data
2.10.2-3	Allowable Stresses in Closure Bolts For Normal Conditions
2.10.2-4	Allowable Stresses in Closure Bolts For Accident Conditions
2.10.2-5	Design Parameters for Ram Port Cover Bolt Analysis

APPENDIX 2.10.2

NUHOMS®-MP197 CASK LID BOLT ANALYSIS

2.10.2.1 Introduction

This section evaluates the ability of the transport cask closure to maintain a leak tight seal under normal and accident conditions. Also evaluated in this section, are the bolt thread and internal thread stresses, and lid bolt fatigue. The stress analysis is performed in accordance with NUREG/CR-6007 [1].

The NUHOMS®-MP197 cask lid closure arrangement is shown in Appendix 1.4, Drawing 1093-71-7. The 4.5 inch thick lid is bolted directly to the end of the containment vessel flange by 48 high strength alloy steel 1.50 inch diameter bolts. Close fitting alignment pins ensure that the lid is centered in the vessel.

The lid bolt is shown in Appendix 1.4, Drawing 1093-71-7. The bolt material is SA-540 Gr. B24 class 1 which has a minimum yield strength of 150 ksi at room temperature [2].

The following ways to minimize bolt forces and bolt failures for shipping casks are taken directly from NUREG/CR-6007, page xiii [1]. All of the following design methods are employed in the NUHOMS®-MP197 cask closure system.

- Protect closure lid from direct impact to minimize bolt forces generated by free drops. (use impact limiters)
- Use materials with similar thermal properties for the closure bolts, the lid, and the cask wall to minimize the bolt forces generated by fire accident
- Apply sufficiently large bolt preload to minimize fatigue and loosening of the bolts by vibration.
- Lubricate bolt threads to reduce required preload torque and to increase the predictability of the achieved preload.
- Use closure lid design which minimizes the prying actions of applied loads.
- When choosing a bolt preload, pay special attention to the interactions between the preload and thermal load and between the preload and the prying action.

The following evaluations are presented in this section:

- Lid bolt torque
- Bolt preload
- Gasket seating load
- Pressure load
- Temperature load
- Impact load
- Puncture load
- Thread engagement length evaluation
- Bearing stress
- Load combinations for normal and accident conditions
- Bolt stresses and allowable stresses
- Lid bolt fatigue

The design parameters of the lid closure are summarized in Table 2.10.2-1. The lid bolt data and material allowables are presented in Tables 2.10.2-2 through 2.10.2-4. A maximum temperature of 200°F is used in the lid bolt region during normal and accident conditions. The following load cases are considered in the analysis.

1. Preload + Temperature Load (normal condition)
2. Pressure Load + 1 Foot Drop (normal condition)
3. Pressure + 30 Foot Corner Drop (accident condition)
4. Pressure + Puncture Load (accident condition)

2.10.2.2 Bolt Load Calculations

Symbols and terminology used in this analysis are taken from NUREG/CR-6007 [1] and are reproduced in Table 2.10.2-1.

2.10.2.2.1 Lid Bolt Torque

A bolt torque range of 1,440 to 1,510 ft. lb. has been selected. Using the minimum torque,

$$F_a = Q/KD_b = 1,440 \times 12 / (0.1 \times 1.500) = 115,200 \text{ lb.}, \text{ and}$$

$$\text{Preload stress} = F_a / \text{Stress Area (Table 2.10.2-2)} = 115,200 / 1.404 = 82,050 \text{ psi.}$$

Using the maximum torque,

$$F_a = Q/KD_b = 1,510 \times 12 / (0.1 \times 1.500) = 120,800 \text{ lb.}, \text{ and}$$

$$\text{Preload stress} = F_a / \text{Stress Area (Table 2.10.2-2)} = 120,800 / 1.404 = 86,040 \text{ psi.}$$

2.10.2.2.2 Bolt Preload ([1], Table 4.1)

For the maximum torque of 1,510 ft. lb.,

$$F_a = 120,800 \text{ lb.}, \text{ and}$$

For the minimum torque of 1,440 ft. lb.,

$$F_a = 115,200 \text{ lb.}, \text{ and}$$

Residual torsional moment for minimum torque of 1,440 ft. lb. is,

$$M_{tr} = 0.5Q = .5(1,440 \times 12) = 8,640 \text{ in. lb.}$$

Residual torsional moment for maximum torque of 1,510 ft. lb. is,

$$M_{tr} = 0.5Q = .5(1,510 \times 12) = 9,060 \text{ in. lb.}$$

Residual tensile bolt force for maximum torque,

$$F_{ar} = F_a = 120,800 \text{ lb.}$$

2.10.2.2.3 Gasket Seating Load

Since an elastomer o-ring is used, the gasket seating load is negligible.

2.10.2.2.4 Pressure Loads ([1], Table 4.3)

Axial force per bolt due to internal pressure is

$$F_a = \frac{\pi D_{lg}^2 (P_{li} - P_{lo})}{4N_b}$$

D_{lg} for outer seal (conservative) = 69.873 in. Then,

$$F_a = \frac{\pi(69.873^2)(50 - 0)}{4(48)} = 3,994 \text{ lb./bolt.}$$

The fixed edge closure lid force is,

$$F_f = \frac{D_{lb}(P_{li} - P_{lo})}{4} = \frac{72.31(50)}{4} = 904 \text{ lb. in.}^{-1}$$

The fixed edge closure lid moment is,

$$M_f = \frac{(P_{li} - P_{lo})D_{lb}^2}{32} = \frac{50(72.31^2)}{32} = 8,170 \text{ in. lb. in.}^{-1}.$$

The shear bolt force per bolt is,

$$F_s = \frac{\pi E_l t_l (P_{li} - P_{lo}) D_{lb}^2}{2 N_b E_c t_c (1 - N_{ul})} = \frac{\pi (27.8 \times 10^6) (4.5) (50) (72.31)^2}{2 (48) (27.6 \times 10^6) (7.0) (1 - 0.305)} = 7,971 \text{ lb./bolt.}$$

The lid shoulder takes this shear force, so that $F_s = 0$.

2.10.2.2.5 Temperature Loads

From reference 4, the lid bolt material is SA-540, Type B24, class 1, 2Ni 3/4Cr 1/3Mo. The Lid is made of SA-693 Type 630, or SA-705 Type 630, both of which are 17Cr 4Ni 4Cu. The Cask Flange is constructed from SA-182 Type FXM-19, which is 22Cr 13Ni 5Mn. Therefore, the bolts have a coefficient of thermal expansion of 6.7×10^{-6} in./in. $^{\circ}\text{F}^{-1}$ at 200 $^{\circ}$ F, the lid has a coefficient of thermal expansion of 5.90×10^{-6} in./in. $^{\circ}\text{F}^{-1}$ at 200 $^{\circ}$ F, and the flange has a coefficient of thermal expansion of 8.5×10^{-6} in./in. $^{\circ}\text{F}^{-1}$ at 200 $^{\circ}$ F [2].

$$F_a = 0.25 \pi D_b^2 E_b (a_l T_l - a_b T_b)$$

$$F_a = 0.25(\pi)(1.500^2)(27.1 \times 10^6)[(5.90 \times 10^{-6})(130) - (6.7 \times 10^{-6})(130)] = -4,981 \text{ lb.}$$

Even though the lid and flange are constructed from different materials, the shear force per bolt, F_s , due to a temperature change of 130 $^{\circ}$ F is, 0 psi, since the clearance holes in the lid are oversized (1.69 in. diameter) allowing the lid to grow in the radial direction.

$$F_s = 0.$$

The temperature difference between the inside of the lid and the outside of the lid will always be less than one degree. Consequently, the resulting bending moment is negligible.

$$M_f = 0.$$

2.10.2.2.6 Impact Loads ([1], Table 4.5)

The non-prying tensile bolt force per bolt, F_a , is,

$$F_a = \frac{1.34 \sin(xi)(DLF)(ai)(W_l + W_c)}{N_b} = \frac{1.34 \sin(xi)(1.1)(ai)(96,000)}{48} = 2,948(ai) \sin(xi) \text{ lb./bolt.}$$

Note: $W_l + W_c$ is conservatively assumed to be 96,000 lbs. [Actual weight from Section 2.2 = 5,611 (lid) + 22,918 (basket and hold down ring) + 22,467 (canister) + 43,005 (fuel assemblies) = 94,001 lbs.]

The shear bolt force is,

$$F_s = \frac{\cos(xi)(ai)(W_l)}{N_b} = \frac{6,000(ai) \cos(xi)}{48} = 125(ai) \cos(xi) \text{ lb./bolt.}$$

The lid shoulder during normal and accident condition drops takes shear force. Therefore,

$$F_s = 0.$$

The fixed-edge closure lid force, F_f , is,

$$F_f = \frac{1.34 \sin(xi)(DLF)(ai)(W_l + W_c)}{\pi D_{lb}} = \frac{1.34 \sin(xi)(1.1)(ai)(96,000)}{\pi(72.31)} = 622.9 \sin(xi)(ai) \text{ lb. in.}^{-1}$$

The fixed-edge closure lid moment, M_f , is,

$$M_f = \frac{1.34 \sin(xi)(DLF)(ai)(W_l + W_c)}{8\pi} = \frac{1.34 \sin(xi)(1.1)(ai)(96,000)}{8\pi} = 5,630 \sin(xi)(ai) \text{ in.lb.in.}^{-1}$$

Normal Condition Loads

Even though the 1 foot side drop is the only credible normal condition impact event, all 1 foot drop orientations are conservatively considered for the lid bolt analysis. Since the bolts are protected by the impact limiter during a 90° end drop, the worst case scenario is taken to be roughly a 60° C.G. over corner drop. From the impact limiter 1 foot normal condition analysis (Appendix 2.10.8, Table 2.10.8-13), the maximum axial g load for a 1 foot 60° corner drop is 5 gs . Since the axial acceleration is used, xi is taken to be 90°.

$$ai = 5 \text{ gs, and } xi = 90^\circ$$

Therefore,

$$\begin{aligned} F_a &= 2,948 \times 5 \times \sin(90^\circ) = 14,740 \text{ lb./bolt,} \\ F_s &= 0 \text{ lb./bolt,} \\ F_f &= 622.9 \times 5 \times \sin(90^\circ) = 3,115 \text{ lb./bolt, and} \\ M_f &= 5,630 \times 5 \times \sin(90^\circ) = 28,150 \text{ lb./bolt.} \end{aligned}$$

Accident Condition Loads

The accident condition impact load is taken to be the axial acceleration due to a 30 foot, 60° corner drop (Appendix 2.10.8). Since the axial acceleration is used, xi is taken to be 90°.

$$ai = 34 \text{ gs, and } xi = 90^\circ$$

Therefore,

$$\begin{aligned} F_a &= 2,948 \times 34 \times \sin(90^\circ) = 100,232 \text{ lb./bolt,} \\ F_s &= 0 \text{ lb./bolt,} \\ F_f &= 622.9 \times 34 \times \sin(90^\circ) = 21,179 \text{ lb./bolt, and} \\ M_f &= 5,630 \times 34 \times \sin(90^\circ) = 191,420 \text{ lb./bolt.} \end{aligned}$$

Puncture Loads ([1], Table 4.7):

The non-prying tensile bolt force per bolt, F_a , is,

$$F_a = \frac{-\sin(xi) Pun}{N_b},$$

where,

$$P_{un} = \text{The smaller of } \begin{cases} 0.75\pi D_{pb}^2 S_{yl} \\ 0.6\pi D_{pb} t_l S_{ul} \\ 0.25\pi D_{pb} S_{fjb}^* \end{cases}$$

*Flow stress of puncture bar (45 ksi. for mild steel).

$$= \text{The smaller of } \begin{cases} 0.75\pi(6^2)(106,300) = 9.017 \times 10^6 \\ 0.6\pi(6)(9.5)(140,000) = 7.125 \times 10^6 \\ 0.25\pi(6^2)(45,000) = 1.272 \times 10^6 \end{cases}$$

$$\Rightarrow p_{un} = 1.272 \times 10^6 \text{ lb.}$$

The puncture force is greatest when $\xi = 90^\circ$. Conservatively neglect the protection provided by the impact limiter. Then,

$$F_a = \frac{-\sin(\xi)1.272 \times 10^6}{48} = -26,510 \text{ lb.}$$

Since this force is negative (inward acting), the actual resulting bolt force, $F_a = 0$, because the applied load is supported by the cask wall and not the lid bolts. The shear bolt force is,

$$F_s = \frac{\cos(90^\circ)P_{un}}{N_b} \text{ lb./bolt.}$$

The lid shoulder during puncture takes shear force. Therefore,

$$F_s = 0.$$

The fixed-edge closure lid force, F_f , is,

$$F_f = \frac{-\sin(\xi)P_{un}}{\pi D_{lb}} = \frac{-\sin(90^\circ)1.272 \times 10^6}{\pi(72.31)} = -5,601 \text{ lb.in}^{-1}.$$

The fixed-edge closure lid moment, M_f , is,

$$M_f = \frac{-\sin(\xi)P_{un}}{4\pi} = \frac{-\sin(90^\circ)1.272 \times 10^6}{4\pi} = -101,250 \text{ lb.in}^{-1}.$$

LID BOLT INDIVIDUAL LOAD SUMMARY

Load Case	Applied Load		Non-Prying Tensile Force, F_a (lb.)	Torsional Moment, M_t (in. lb.)	Prying Force, F_f (lb.in. ⁻¹)	Prying Moment, M_f (in. lb. in. ⁻¹)
Preload	Residual	Maximum Torque	120,800	9,060	0	0
		Minimum Torque	115,200	8,640	0	0
Gasket	Seating Load		0	0	0	0
Pressure	50 psig Internal		3,994	0	904	8,170
Thermal	300°F		-4,981	0	0	0
Impact	1 Foot Normal Condition Drop (5 gs)		14,740	0	3,115	28,150
	30 foot Accident Condition Drop (34 gs)		100,200	0	21,180	191,400
Puncture	Drop on six inch diameter rod		0	0	-5,601	-101,250

2.10.2.3 Load Combinations ([1], Table 4.9)

A summary of normal and accident condition load combinations is presented in the following table.

LID BOLT NORMAL AND ACCIDENT LOAD COMBINATIONS

Load Case	Combination Description		Non-Prying Tensile Force, F_a (lb.)	Torsional Moment, M_t (in. lb.)	Prying Force, F_f (lb.in. ⁻¹)	Prying Moment, M_f (in. lb. in. ⁻¹)
1.	Preload + Temperature (Normal Condition)	A. Maximum Torque	115,800	9,060	0	0
		B. Minimum Torque	110,200	8,640	0	0
2.	Pressure + Normal Impact (Normal Condition)		18,730	0	4,019	36,320
3.	Pressure + Accident Impact (Accident Condition)		104,200	0	22,080	199,600
4.	Pressure + Puncture (Accident Condition)		3,994	0	-4,697	-93,080

Additional Prying Bolt Force

Since the prying forces applied in load case 4 (pressure + puncture) acts inward, normal to the cask lid, an additional prying bolt force, F_{ap} , is generated (Ref. 1, Table 2.1). No additional force is generated for the outward loadings however (load cases 1, 2, and 3), because of the gap between the lid and flange at the outer edge. F_{ap} is calculated in the following way.

$$F_{ap} = -\left(\frac{\pi D_{lb}}{N_b}\right) \left[\frac{\frac{2M_f}{(D_{lo}^* - D_{lb})} - C_1(B - F_f) - C_2(B - P)}{C_1 + C_2} \right],$$

where,

$$C_1 = 1, C_2 = \left(\frac{8}{3(D_{lo}^* - D_{lb})^2} \right) \left[\frac{E_t t_l^3}{1 - N_{ul}} + \frac{(D_{lo} - D_{li}) E_f t_f^3}{D_{lb}} \right] \left(\frac{L_b}{N_b D_b^2 E_b} \right)$$

*Applicable for outward load only, for negative M_f , replace D_{lo} with D_{li} .

$$= \left(\frac{8}{3(68.42 - 72.31)^2} \right) \left[\frac{27.8 \times 10^6 (4.5^3)}{1 - 0.3} + \frac{(74.68 - 68.42)(27.6 \times 10^6)(7.0)^3}{72.31} \right] \left(\frac{2.27}{(48)(1.500^2)(27.1 \times 10^6)} \right)$$

$$= 0.607,$$

B is the non-prying tensile bolt force, and P is the bolt preload. Since $F_s = 0$, $F_s < P$, and therefore $B = P$. Parameters B , P , F_f , and M_f are quantities per unit length of bolt circle. For the applied inward force,

$$P = B = \frac{F_a N_b}{\pi D_{lb}} = \frac{(110,200)(48)}{\pi(72.31)} = 23,280 \text{ lb. in.}^{-1},$$

$$M_f = -101,250 \text{ in.lb. in.}^{-1}, \text{ and } F_f = 0 \text{ lb. in.}^{-1}.$$

Therefore,

$$F_{ap} = \left(\frac{\pi(72.31)}{48} \right) \left[\frac{2(-101,250) - 1(23,280 - 0) - 0.607(23,280 - 23,280)}{68.42 - 72.31} \right] \frac{1}{1 + 0.607}$$

$$= 84,750 \text{ lb./bolt.}$$

It is observed that the additional tensile bolt force due to prying for the puncture is less than the accident impact force. The puncture is therefore not critical for bolt stress evaluation.

Bolt Bending Moment ([1], Table 2.2)

The maximum bending bolt moment, M_{bb} , generated by the applied load is evaluated as follows:

$$M_{bb} = \left(\frac{\pi D_{lb}}{N_b} \right) \left[\frac{K_b}{K_b + K_l} \right] M_f$$

The K_b and K_l are based on geometry and material properties and are defined in NUREG/CR-6007 [1], Table 2.2. By substituting the values given above,

$$K_b = \left(\frac{N_b}{L_b} \right) \left(\frac{E_b}{D_{lb}} \right) \left(\frac{D_b^4}{64} \right) = \left(\frac{48}{4.0} \right) \left(\frac{27.1 \times 10^6}{72.31} \right) \left(\frac{1.500^4}{64} \right) = 3.557 \times 10^5, \text{ and}$$

$$K_l = \frac{E_l t_l^3}{3 \left[(1 - N_{ul}^2) + (1 - N_{ul})^2 \left(\frac{D_{lb}}{D_{lo}} \right)^2 \right] D_{lb}} = \frac{27.8 \times 10^6 (4.5^3)}{3 \left[(1 - 0.305^2) + (1 - 0.305)^2 \left(\frac{72.31}{74.68} \right)^2 \right] 72.31}$$

$$= 8.588 \times 10^6$$

Therefore,

$$M_{bb} = \left(\frac{\pi 72.31}{48} \right) \left[\frac{3.557 \times 10^5}{3.557 \times 10^5 + 8.588 \times 10^6} \right] M_f = 0.1882 M_f$$

For load case 2, $M_f = 36,320$ in. lb. Substituting this value into the equation above gives,

$$M_{bb} = 6,836 \text{ in. lb. / bolt.}$$

2.10.2.4 Bolt Stress Calculations ([1], Table 5.1)

2.10.2.4.1 Average Tensile Stress

The bolt preload is calculated to withstand the worst case load combination and to maintain a clamping (compressive) force on the closure joint, under both normal and accident conditions. Based upon the load combination results (see Table LID BOLT NORMAL AND ACCIDENT LOAD COMBINATIONS on page 8), it is shown that a positive (compressive) load is maintained on the clamped joint for all load combinations. Therefore, in both normal and accident load cases, the maximum non-prying tensile force of 120,800 lb., from the maximum torque individual load case, is used. The temperature load is conservatively neglected since it tends to decrease the applied bolt load.

Normal Condition

$$S_{ba} = 1.2732 \frac{F_a}{D_{ba}^2} = 1.2732 \frac{120,800}{1.337^2} = 86,040 \text{ psi.} = 86.0 \text{ ksi.}$$

Accident Condition

$$S_{ba} = 1.2732 \frac{120,800}{1.337^2} = 86,040 \text{ psi.} = 86.0 \text{ ksi.}$$

2.10.2.4.2 Bending Stress

Normal Condition

$$S_{bb} = 10.186 \frac{M_{bb}}{D_{ba}^3} = 10.186 \frac{6,836}{1.337^3} = 29,340 \text{ psi.} = 29.3 \text{ ksi.}$$

2.10.2.4.3 Shear Stress

For both normal and accident conditions, the average shear stress caused by shear bolt force F_s is,

$$S_{bs} = 0.$$

For normal and accident conditions the maximum shear stress caused by the torsional moment M_t is,

$$S_{bt} = 5.093 \frac{M_t}{D_{ba}^3} = 5.093 \frac{9,060}{1.337^3} = 19,310 \text{ psi.} = 19.3 \text{ ksi.}$$

2.10.2.4.4 Maximum Combined Stress Intensity

The maximum combined stress intensity is calculated in the following way ([1], Table 5.1).

$$S_{bi} = [(S_{ba} + S_{bb})^2 + 4(S_{bs} + S_{bt})^2]^{0.5}$$

For normal conditions combine tension, shear, bending, and residual torsion.

$$S_{bi} = [(86,040 + 29,130)^2 + 4(0 + 19,310)^2]^{0.5} = 121,500 \text{ psi.} = 121.5 \text{ ksi.}$$

2.10.2.4.5 Stress Ratios

In order to meet the stress ratio requirement, the following relationship must hold for both normal and accident conditions.

$$R_t^2 + R_s^2 < 1$$

Where R_t is the ratio of average tensile stress to allowable average tensile stress, and R_s is the ratio of average shear stress to allowable average shear stress.

For normal conditions

$$R_t = 86,040/95,600 = 0.931,$$

$$R_s = 19,310/57,400 = 0.349,$$

$$R_t^2 + R_s^2 = (0.900)^2 + (0.336)^2 = 0.923 < 1.$$

For accident conditions

$$R_t = 86,040/115,500 = 0.745,$$

$$R_s = 19,310/69,300 = 0.279,$$

$$R_t^2 + R_s^2 = (0.745)^2 + (0.279)^2 = 0.633 < 1.$$

2.10.2.4.6 Bearing Stress (Under Bolt Head)

The maximum axial bolt force is 120,800 lb. The lid bolt head is a 2.25 inch diameter socket head. The diameter of the bolt hole in the NUHOMS[®]-MP197 cask lid is 1.69 inches. Therefore the bearing area, A, under the lid bolt head is,

$$A = (\pi/4)(2.25^2 - 1.69^2) = 1.733 \text{ in}^2.$$

The bearing stress is,

$$\text{Bearing Stress} = 120,800/1.733 = 69,706 \text{ psi.} = 69.7 \text{ ksi.}$$

The allowable bearing stress on the lid is taken to be the yield stress of the lid material at 300° F. The lid may be manufactured out of SA-693 TP630 or SA-705 TP630. The minimum yield strength of both materials at 300° F is 101,800 psi.

2.10.2.5 Analysis Results

A summary of the bolt stresses calculated above is presented in the following table:

SUMMARY OF STRESSES AND ALLOWABLES

Stress Type	Normal Condition		Accident Condition	
	Stress	Allowable	Stress	Allowable
Average Tensile (ksi.)	86.0	95.6	86.0	115.5
Shear (ksi)	19.3	57.4	19.3	69.3
Combined (ksi)	121.5	129.1	Not Required [1]	
Interaction E.Q. $R_t^2 + R_s^2 < 1$	0.923	1	0.633	1
Bearing (ksi) Allowable (ksi) (S _y of lid material)	69.7	106.3	Not Required [1]	

The calculated bolt stresses are all less than the specified allowable stresses.

2.10.2.6 Fatigue Analysis

The purpose of the fatigue analysis is to show quantitatively that the fatigue damage to the bolts during normal conditions of transport is acceptable. This is done by determining the fatigue usage factor for each normal transport event. For this analysis it is assumed that the transport cask lid bolts are replaced after 85 round trip shipments. The total cumulative damage or fatigue usage for all events is conservatively determined by adding the usage factors for the individual events. The sum of the individual usage factors is checked to make certain that for the 85 round trip shipments of the NUHOMS[®]-MP197 cask, the total usage factor is less than one. The following sequence of events is assumed for the fatigue evaluation.

1. Operating Preload
2. Pressure and Temperature Fluctuations
3. Road vibration
4. Shock
5. Test Pressure
6. 1 foot normal condition drop

Since the bolt preload stress applied to the NUHOMS[®]-MP197 cask lid bolts is higher than all of the other normal and accident condition loads, the stress in the bolt will never exceed the bolt preload stress. Consequently, the application and removal of preload is the only real cyclic loading that occurs in the lid bolts. The following analysis is therefore very conservative since it assumes that the usage factor is the sum of all of the individual event usage factors, and not simply the usage factor for bolt preload.

2.10.2.6.1 Operating Preload

Assuming that the bolts are replaced after 85 round trips, the number of preload cycles is two times the number trips or 170 cycles.

The maximum tensile stress due to bolt preload is 86,040 psi, and the maximum shear stress due to residual bolt torsion is 19,310 psi. The corresponding stress intensity is then

$$S.I. = \sqrt{86,040^2 + 4(19,310^2)} = 94,310 \text{ psi.}$$

2.10.2.6.2 Test Pressure

The hydrostatic test pressure, according to Reference 3, is 1.25×50 psi. (design pressure), or 62.5 psi., and will only be performed once. Reference 1 provides bolt loads due to 50 psi internal pressure. So for 62.5 psi pressure, the bolt loads are the following.

$$F_a = 3994 \times (62.5/50) = 11,993 \text{ lb./ bolt.}$$

$$F_s = 0 \times (62.5/50) = 0 \text{ lb. / bolt.}$$

$$F_f = 904 \times (62.5/50) = 1,130 \text{ lb.in.}^{-1}$$

$$M_f = 8170 \times (62.5/50) = 10,213 \text{ in.lb.in.}^{-1}$$

$$M_{bb} = 0.1895 M_f \text{ in.lb. / bolt.}$$

The minimum lid bolt diameter is 1.337 in. Therefore from NUREG/CR-6007 [1], we get the following

$$S_{ba} = 1.2732 \frac{F_a}{D_{ba}^2} = 1.2732 \frac{4,993}{1.337^2} = 2,556 \text{ psi.},$$

$$S_{bb} = 10.186 \frac{M_{bb}}{D_{ba}^3} = 10.186 \frac{0.1895(10,213)}{1.337^3} = 8,248 \text{ psi.},$$

Since internal pressure causes no bolt torsion, and all shear loads are taken by the lid shoulder,

$$S_{bs} = 0, \text{ and } S_{bt} = 0.$$

$$S.I. = S_{bi} = [(S_{ba} + S_{bb})^2 + 4(S_{bs} + S_{bt})^2]^{0.5} = [(3,556 + 8,248)^2 + 4(0)^2]^{0.5} = 11,805 \text{ psi.}$$

2.10.2.6.3 Vibration / Shock

Since the NUHOMS[®]-MP197 cask may be shipped either by truck or by rail car, the shock loading for both cases will be considered.

Truck Shock

Shock input was obtained from ANSI N14.23 [4]. This standard specifies shock loads that correspond to normal transport over rough roads or minor accidents such as backing into a loading dock. Since the NUHOMS[®]-MP197 cask will be transported on interstate highways or major good roads, the shock loads will not be applied continuously to the normal transport mode for the package. The fatigue calculation assumes an average trip of 3,000 miles averaging 45 miles per hour. The total driving time would then be 3,000 miles / 45 mph. = 67 hours. Assume the driver stops and leaves the interstate every 4 hours and assume that one shock could be experienced during each of these stops. The return trip package behavior is assumed to be the same as the "loaded" trip even though the cargo is no longer present. Therefore shock loading occurs 18 (shocks per trip) × 2 (round trip) × 85 shipments = 3,060 cycles.

ANSI N14.23 [4] specifies a peak shock loading of 2.3 gs in the longitudinal direction. The weight of the lid, basket, canister, and fuel assemblies is conservatively assumed to be 95,000 lb. The actual maximum weight of the lid, basket, and canister is 94,001 lb. (Section 2.2). The bolt force due to truck shock is,

$$(95,000 \text{ lb})(2.3 \text{ gs}) / (48 \text{ bolts})(1.404 \text{ in}^2 \text{ per bolt}) = 3,242 \text{ psi.}$$

Rail Car Shock

Again, assume 85 round trip shipments, averaging 3,000 miles each way. NUREG 766510 [5] reports that there are roughly 9 shock cycles per 100 miles of rail car transport. Therefore the total number of cycles is $3,000 \text{ (miles)} \times 2 \text{ (round trip)} \times 85 \text{ (shipments)} \times 0.09 \text{ (Shocks per mile)} = 45,900 \text{ cycles}$.

NUREG 766510 [5] specifies a peak shock loading of 4.7 gs in the longitudinal direction for rail car transport. Consequently, the bolt force due to rail car shock is

$$(95,000 \text{ lb})(4.7 \text{ gs}) / (48 \text{ bolts})(1.404 \text{ in}^2 \text{ per bolt}) = 6,625 \text{ psi.}$$

Vibration

Since vibration accelerations are higher on a truck than on a rail car, the truck vibration loads are considered bounding. According to ANSI N14.23 [4], the peak vibration load at the bed of a truck in the longitudinal direction is 0.3 g's. This results in a stress of 423 psi, which is negligible for a high strength bolt.

2.10.2.6.4 Pressure and Temperature Fluctuations

The following bolt loads result from the maximum temperature change of 230° F (Section 2.10.2.2.5)

$$F_a = -10,850 \text{ lb./ bolt.}$$

$$F_s = 0 \text{ lb. / bolt.}$$

$$F_f = 0 \text{ lb.in.}^{-1}$$

$$M_f = 0 \text{ in.lb.in.}^{-1}$$

Since the temperature load tends to reduce the axial load in the lid bolts, the temperature load is conservatively neglected. The maximum pressure difference between in the inside and the outside of the lid is conservatively taken to be 50 psi. The bolt loads due to this pressure difference are (Section 2.10.2.2.4),

$$F_a = 3,994 \text{ lb./ bolt.}$$

$$F_s = 0 \text{ lb./ bolt.}$$

$$F_f = 904 \text{ lb.in.}^{-1}$$

$$M_f = 8,170 \text{ in.lb.in.}^{-1}$$

$$M_{bb} = 0.1895 M_f \text{ in.lb. / bolt.}$$

The minimum lid bolt diameter is 1.337 in. The tensile and bending stresses in the lid bolts, generated by pressure fluctuations, are the following [1].

$$S_{ba} = 1.2732 \frac{F_a}{D_{ba}^2} = 1.2732 \frac{3,994}{1.337^2} = 2,845 \text{ psi.},$$

$$S_{bb} = 10.186 \frac{M_{bb}}{D_{ba}^3} = 10.186 \frac{0.1895(8,170)}{1.337^3} = 6,598 \text{ psi.}$$

Since internal pressure and temperature loads cause no bolt torsion, and all shear loads are taken by the lid shoulder,

$$S_{bs} = 0, \text{ and } S_{bt} = 0.$$

The stress intensity due the combine temperature and pressure fluctuations is as follows.

$$S.I. = S_{bi} = [(S_{ba} + S_{bb})^2 + 4(S_{bs} + S_{bt})^2]^{0.5} = [(2,845 + 6,598)^2 + 4(0)^2]^{0.5} = 9,443 \text{ psi.}$$

Assuming this cycle occurs once each one way shipment, the total number of pressure and temperature fluctuation cycles is 170.

2.10.2.6.5 1 Foot Normal Condition Drop

The normal condition drop consists of a 1 foot drop in an orientation that results in the most damage. For the side drop the resulting shear load is taken entirely by the lid / flange interface. For the end drop, the load is transferred to the cask body via the impact limiters, protecting the bolts. Therefore the worst case scenario is taken to be roughly a 60° C.G. over corner drop. From Section 2.10.2.2.6, the resulting bolt loading is the following.

$$\begin{aligned} F_a &= 14,740 \text{ lb./bolt,} \\ F_s &= 0 \text{ lb./bolt,} \\ F_f &= 3,115 \text{ lb./bolt, and} \\ M_f &= 28,150 \text{ lb./bolt.} \\ M_{bb} &= 0.1895 M_f. \end{aligned}$$

The tensile and bending bolt stresses generated are the following.

$$S_{ba} = 1.2732 \frac{F_a}{D_{ba}^2} = 1.2732 \frac{14,740}{1.337^2} = 10,499 \text{ psi.},$$

$$S_{bb} = 10.186 \frac{M_{bb}}{D_{ba}^3} = 10.186 \frac{0.1896(28,150)}{1.337^3} = 22,747 \text{ psi,}$$

Since the impact load causes no bolt torsion, and all shear loads are taken by the lid shoulder,

$$S_{bs} = 0, \text{ and } S_{bt} = 0.$$

$$S.I. = S_{bi} = [(S_{ba} + S_{bb})^2 + 4(S_{bs} + S_{bt})^2]^{0.5} = [(10,499 + 22,747)^2 + 4(0)^2]^{0.5} = 33,246 \text{ psi.}$$

Conservatively assume that the cask is dropped once per shipment, resulting in 85 normal condition drops before the lid bolts are changed.

2.10.2.6.6 Damage Factor Calculation

The following damage factors are computed based on the stresses and cyclic histories described above, a fatigue strength reduction factor, K_F , of 4 [6], and the fatigue curve shown in Table I-9.4 of ASME Section III Appendices.

Event	Stress Intensity (psi.)	S.I. $\times K_F$ (psi.)	S_a (psi.)	Cycles		Damage Factor n/N
				n	N	
Operating Preload	94,310	377,240	211,933	170	250	0.68
Test Pressure	11,804	47,216	26,526	85	20,000	0.00
Truck Shock	3,242	12,968	7,285	3,060	∞	0.00
Rail Car Shock	6,625	26,500	14,888	45,900	300,000	0.15
Pressure and Temperature	9,443	37,772	21,220	170	50,000	0.00
1 Foot Drop Impact Load	33,246	132,984	74,710	85	1,500	0.06
Σ						0.90

Here, n is the number of cycles, N is taken from Figure I-9.4 of reference 7, and S_a is defined in the following way.

If one cycle goes from 0 to $+S.I.$, then $S_a = (1/2) \times S.I. \times K_F \times K_E$.

If one cycle goes from $-S.I.$ to $+S.I.$, then $S_a = S.I. \times K_F \times K_E$.

Where, K_E is the correction factor for modulus of elasticity. The Modulus of Elasticity of SA-540, Grade B24, Class 1 is 26.7×10^6 psi. @ 300° F. Therefore, $K_E = 30.0 \times 10^6 / 26.7 \times 10^6 = 1.1236$ [7] [2].

2.10.2.7 Minimum Engagement Length for Bolt and Flange

For a 1 1/2" – 6UNC – 2A bolt, the material is SA-540 GR. B24 CL.1, with

$$S_u = 165 \text{ ksi.}, \text{ and}$$

$$S_y = 150 \text{ ksi (at room temperature)}$$

The threaded insert material is constructed from type 304 stainless steel [9] and have the following material properties.

$$S_u = 70 \text{ ksi.}, \text{ and}$$

$$S_y = 30 \text{ ksi (at room temperature)}$$

The minimum engagement length, L_e , for the bolt and flange is ([8], Page 1149),

$$L_e = \frac{2A_t}{3.1416K_{n \max} \left[\frac{1}{2} + .57735n(E_{s \min} - K_{n \max}) \right]}$$

Where,

A_t = tensile stress area = 1.404 in.²,

n = number of threads per inch = 6,

$K_{n \max}$ = maximum minor diameter of internal threads = 1.350 in. ([8], p. 1292)

$E_{s \min}$ = minimum pitch diameter of external threads = 1.3812 in. ([8], p. 1292)

Substituting the values given above,

$$L_e = \frac{2(1.404)}{(3.1416)1.350 \left[\frac{1}{2} + .57735(6)(1.3812 - 1.350) \right]} = 1.089 \text{ in.}$$

$$J = \frac{A_s \times S_{ue}}{A_n \times S_{ui}} \quad [4]$$

Where, J is a factor for the relative strength of the external and internal threads, S_{ue} is the tensile strength of external thread material, and S_{ui} is the tensile strength of internal thread material.

A_s = shear area of external threads = $3.1416 n L_e K_{n \max} [1/(2n) + .57735 (E_{s \min} - K_{n \max})]$

A_n = shear area of internal threads = $3.1416 n L_e D_{s \min} [1/(2n) + .57735(D_{s \min} - E_{n \max})]$

For the bolt / Helicoil insert connection:

$$E_{n \max} = \text{maximum pitch diameter of internal threads} = 1.4022 \text{ in. ([8], p. 1294).}$$

$$D_{s \min} = \text{minimum major diameter of external threads} = 1.4794 \text{ in. ([8], p. 1292)}$$

Therefore,

$$A_s = 3.1416(6)(1.089)(1.350)[1/(2 \times 6) + .57735 (1.3812 - 1.350)] = 2.808 \text{ in.}^2$$

$$A_n = 3.1416(6)(1.089)(1.4794)[1/(2 \times 6) + .57735 (1.4794 - 1.4022)] = 3.883 \text{ in.}^2$$

So,

$$J = \frac{2.808(165.0)}{3.883(70.0)} = 1.705$$

The required length of engagement, Q , to prevent stripping of the internal threads is,

$$Q = L_e J = (1.089)(1.705) = 1.857 \text{ in.}$$

The actual minimum engagement length = 2.25 in. > 1.857 in. (limited by threaded insert length).

2.10.2-8 Ram Port Cover Bolt Analysis

This section evaluates the ability of the ram port closure to maintain a leak tight seal under normal and accident conditions. Also evaluated in this section, are the ram port cover bolt thread and internal thread stresses. The stress analysis is performed in accordance with NUREG/CR-6007 [1].

The NUHOMS[®]-MP197 cask ram port closure arrangement is shown in Appendix 1.4, Drawing 1093-71-6. The ram port cover plate is bolted directly to the end of the containment vessel flange by 12 high strength alloy steel 1.00 inch diameter bolts.

The following evaluations are presented in this section:

- Lid bolt torque
- Bolt preload
- Gasket seating load
- Pressure load
- Temperature load
- Impact load
- Puncture load
- Thread engagement length evaluation
- Bearing stress
- Load combinations for normal and accident conditions
- Bolt stresses and allowable stresses

The design parameters of the ram port cover are summarized in Table 2.10.2-5. The ram port cover bolt data and material allowables are presented in Tables 2.10.2-2 through 2.10.2-4. A maximum temperature of 300°F is used in the lid bolt region during normal and accident conditions. The following load cases are considered in the analysis.

5. Preload + Temperature Load (normal condition)
6. Pressure Load + 1 Foot Drop (normal condition)
7. Pressure + 30 Foot Corner Drop (accident condition)
8. Pressure + Puncture Load (accident condition)

2.10.2.8.1 Bolt Load Calculations

Symbols and terminology for this analysis are taken from reference 1 and are reproduced in Table 1.

Lid Bolt Torque and Bolt Preload

A bolt torque range of 100 to 125 ft. lb. has been selected. Using the minimum torque,

$$F_a = Q/KD_b = 100 \times 12 / (0.1 \times 1.00) = 12,000 \text{ lb.}, \text{ and}$$

$$\text{Preload stress} = F_a / \text{Stress Area (Table 2)} = 12,000 / 0.606 = 19,800 \text{ psi.}$$

Using the maximum torque,

$$F_a = Q/KD_b = 125 \times 12 / (0.1 \times 1.00) = 15,000 \text{ lb.}, \text{ and}$$

$$\text{Preload stress} = F_a / \text{Stress Area (Table 2)} = 15,000 / 0.606 = 24,750 \text{ psi.}$$

Residual torsional moment for minimum torque of 100 ft. lb. is,

$$M_{tr} = 0.5Q = .5(100 \times 12) = 600 \text{ in. lb.}$$

Residual torsional moment for maximum torque of 125 ft. lb. is,

$$M_{tr} = 0.5Q = .5(125 \times 12) = 750 \text{ in. lb.}$$

Residual tensile bolt force for maximum torque,

$$F_{ar} = F_a = 15,000 \text{ lb.}$$

Gasket Seating Load (Seal – Parker 2-418, Fluorocarbon, Ref 2):

Since an Elastomer o-ring is used, the gasket seating load is negligible.

Pressure Loads (Ref. 1, Table 4.3):

Axial force per bolt due to internal pressure is

$$F_a = \frac{\pi D_{ig}^2 (P_{ii} - P_{io})}{4N_b}$$

D_{lg} for outer seal (conservative) = 20.02 in. Then,

$$F_a = \frac{\pi(20.02^2)(50-0)}{4(12)} = 1,312 \text{ lb./bolt.}$$

The fixed edge closure lid force is,

$$F_f = \frac{D_{lb}(P_{li} - P_{lo})}{4} = \frac{22.00(50)}{4} = 275 \text{ lb. in.}^{-1}.$$

The fixed edge closure lid moment is,

$$M_f = \frac{(P_{li} - P_{lo})D_{lb}^2}{32} = \frac{50(22.00^2)}{32} = 756 \text{ in. lb. in.}^{-1}.$$

The cask bottom flange shoulder takes the shear force, so that $F_s = 0$.

Temperature Loads:

From reference 3, the lid bolt material is SA-540, Type B24, class 1, 2Ni ¼Cr 1/3Mo. The ram port cover and the cask bottom plate is made of SA-240 Type XM-19, which is 22Cr 13Ni 5Mn. Therefore the bolts have a coefficient of thermal expansion of 6.9×10^{-6} in./in. °F⁻¹ at 300° F, and the flange has a coefficient of thermal expansion of 8.8×10^{-6} in./in. °F⁻¹ at 300° F [2].

$$F_a = 0.25 \pi D_b^2 E_b (a_l T_l - a_b T_b)$$

$$F_a = 0.25(\pi)(1.00^2)(26.7 \times 10^6)[(8.8 \times 10^{-6})(230) - (6.9 \times 10^{-6})(230)] = 9,164 \text{ lb.}$$

Even though the ram port cover and bottom flange are constructed from different materials, the shear force per bolt, F_s , due to a temperature change of 180° F is, 0 psi, since the clearance holes in the cover are oversized (1.63 in. diameter) allowing the cover to grow in the radial direction.

$$F_s = 0.$$

The temperature difference between the inside of the lid and the outside of the lid will always be less than one degree. Consequently, the resulting bending moment is negligible.

$$M_f \approx 0.$$

Impact Loads (Ref. 1, Table 4.5):

During a bottom end drop or bottom corner drop, the cask bottom plate will protect the ram port cover from the inertial load of the cask internals (canister, basket, and fuel). Therefore, the ram port cover bolts will not experience any additional loads during an impact event.

Puncture Loads (Ref. 1, Table 4.7):

The non-prying tensile bolt force per bolt, F_a , is,

$$F_a = \frac{-\sin(xi)Pun}{N_b},$$

where,

$$Pun = \text{The smaller of } \begin{cases} 0.75\pi D_{pb}^2 S_{yl} \\ 0.6\pi D_{pb} t_l S_{ul} \\ 0.25\pi D_{pb} S_{fbb}^* \end{cases}$$

*Flow stress of puncture bar (45 ksi. for mild steel).

$$= \text{The smaller of } \begin{cases} 0.75\pi(6^2)(43,300) = 3.673 \times 10^6 \\ 0.6\pi(6)(2.5)(94,200) = 2.663 \times 10^6 \\ 0.25\pi(6^2)(45,000) = 1.272 \times 10^6 \end{cases}$$

$$\Rightarrow Pun = 1.272 \times 10^6 \text{ lb.}$$

The puncture force is greatest when $xi = 90^\circ$. Conservatively neglect the protection provided by the impact limiter. Then,

$$F_a = \frac{-\sin(xi)1.272 \times 10^6}{12} = -106,030 \text{ lb.}$$

Since this force is negative (inward acting), the actual resulting bolt force, $F_a = 0$, because the applied load is supported by the cask wall and not the lid bolts. The shear bolt force is,

$$F_s = \frac{\cos(90^\circ)Pun}{N_b} \text{ lb./bolt.}$$

The lid shoulder during puncture takes shear force. Therefore,

$$F_s = 0.$$

The fixed-edge closure lid force, F_f , is,

$$F_f = \frac{-\sin(xi)Pun}{\pi D_{lb}} = \frac{-\sin(90^\circ)1.272 \times 10^6}{\pi(22.00)} = -18,410 \text{ lb.in}^{-1}.$$

The fixed-edge closure lid moment, M_f , is,

$$M_f = \frac{-\sin(xi)Pun}{4\pi} = \frac{-\sin(90^\circ)1.272 \times 10^6}{4\pi} = -101,250 \text{ in.lb.in}^{-1}.$$

RAM PORT COVER BOLT INDIVIDUAL LOAD SUMMARY

Load Case	Applied Load		Non-Prying Tensile Force, F_a (lb.)	Torsional Moment, M_t (in. lb.)	Prying Force, F_f (lb.in. ⁻¹)	Prying Moment, M_f (in. lb. in. ⁻¹)
Preload	Residual	Maximum Torque	15,000	750	0	0
		Minimum Torque	12,000	600	0	0
Gasket	Seating Load		0	0	0	0
Pressure	50 psig Internal		1,312	0	275	756
Thermal	250°F		9,164	0	0	0
Impact	1 Foot Normal Condition Drop (5 gs)		0	0	0	0
	30 foot Accident Condition Drop (34 gs)		0	0	0	0
Puncture	Drop on six inch diameter rod		0	0	-18,410	-101,250

2.10.2.8.2 Load Combinations (Ref. 1, Table 4.9):

A summary of normal and accident condition load combinations is presented in the following table.

RAM PORT COVER BOLT NORMAL AND ACCIDENT LOAD COMBINATIONS

Load Case	Combination Description		Non-Prying Tensile Force, F_a (lb.)	Torsional Moment, M_t (in. lb.)	Prying Force, F_f (lb.in. ⁻¹)	Prying Moment, M_f (in. lb. in. ⁻¹)
1.	Preload + Temperature (Normal Condition)	A. Maximum Torque	24,164	750	0	0
		B. Minimum Torque	21,164	600	0	0
2.	Pressure + Normal Impact (Normal Condition)		1,312	0	275	756
3.	Pressure + Accident Impact (Accident Condition)		1,312	0	275	756
4.	Pressure + Puncture (Accident Condition)		1,312	0	-18,130	-100,500

Additional Prying Bolt Force and Bending Bolt Moment (Ref. 1, Table 2.1 and Table 2.2)

Since the prying forces applied in load case 4 (pressure + puncture) acts inward, normal to the cask lid, an additional prying bolt force, F_{ap} , is generated (Ref. 1, Table 2.1). No additional force is generated for the outward loadings however (load cases 1, 2, and 3), because of the gap between the lid and flange at the outer edge (Ref. 3).

Prying forces for the ram port cover plate bolts are determined from FEM analysis, for the puncture load case. The ram port cover is not a full cover plate extending to the diameter of the cask. Therefore, use of NUREG/CR-6007 methodology for calculating the fixed end moments (which is used to calculate prying loads) due to these load conditions is not appropriate for the ram port cover bolts.

A 2-dimensional finite element model is used to compute the ram port cover bolt prying forces caused by the puncture event. Details of the finite element analysis performed are provided in Reference 7.

A single link element is used to represent the ram port cover bolts. Consequently, the resulting force computed in this link element is the total prying force generated in all of the ram port cover bolts. The ram port cover bolt total prying force, computed in reference 7, is 251,360 lb. Therefore, the ram port cover bolt prying force per bolt, F_{ap} , is,

$$F_{ap} = \frac{251,360}{12} = 20,950 \text{ lb./bolt}$$

Since this bolt load is less than the load generated by the minimum bolt preload (21,164 lb./bolt from load case 1B.), the prying force generated by the puncture event is not critical with respect to bolt stress, and will not result in loss of the ram port cover seal.

2.10.2.8.3 Bolt Stress Calculations (Ref. 1, Table 5.1)

Average Tensile Stress:

The bolt preload is calculated to withstand the worst case load combination and to maintain a clamping (compressive) force on the closure joint, under both normal and accident conditions. Based upon the load combination results (see Table RAM PORT COVER BOLT NORMAL AND ACCIDENT LOAD COMBINATIONS), it is shown that a positive (compressive) load is maintained on the clamped joint for all load combinations. Therefore, in both normal and accident load cases, the maximum non-prying tensile force of 24,164 lb., from the maximum torque preload + temperature load case, is used.

Normal Condition:

$$S_{ba} = 1.2732 \frac{F_a}{D_{ba}^2} = 1.2732 \frac{24,164}{0.878^2} = 39,910 \text{ psi.} = 39.9 \text{ ksi.}$$

Accident Condition:

$$S_{ba} = 1.2732 \frac{F_a}{D_{ba}^2} = 1.2732 \frac{24,164}{0.878^2} = 39,910 \text{ psi.} = 39.9 \text{ ksi.}$$

Shear Stress:

For normal and accident conditions the maximum shear stress caused by the torsional moment M_t is,

$$S_{bt} = 5.093 \frac{M_t}{D_{ba}^3} = 5.093 \frac{750}{0.878^3} = 5,644 \text{ psi.} = 5.64 \text{ ksi.}$$

Maximum Combined Stress Intensity:

The maximum combined stress intensity is calculated in the following way (Ref. 1, Table 5.1).

$$S_{bi} = [S_{ba}^2 + 4S_{bt}^2]^{0.5}$$

For normal conditions combine tension, shear, bending, and residual torsion.

$$S_{bi} = [39,910^2 + 4 (5,644)^2]^{0.5} = 41,480 \text{ psi.} = 41.5 \text{ ksi.}$$

2.10.8.2.4 Bearing Stress (Under Bolt Head)

The maximum axial bolt force is 24,164 lb. The ram port cover bolt head is a 1.50 inch diameter socket head. The diameter of the bolt hole in the NUHOMS[®]-MP197 Cask lid is 1.12 inches. Therefore the bearing area, A, under the lid bolt head is,

$$A = (\pi/4)(1.50^2 - 1.12^2) = 0.782 \text{ in}^2.$$

The bearing stress is,

$$\text{Bearing Stress} = 24,164/0.782 = 30,900 \text{ psi.} = 30.9 \text{ ksi.}$$

The allowable bearing stress on the ram port cover is taken to be the yield stress of the cover material at 300° F. The ram port cover is manufactured from SA-240 Type-XM-19 or SA-183 Type FXM-19, which has a yield strength 43.3 psi. @ 300° F.

2.10.2.8.5 Results

A summary of the stresses calculated above is listed in the following table:

SUMMARY OF STRESSES AND ALLOWABLES

Stress Type	Normal Condition		Accident Condition	
	Stress	Allowable	Stress	Allowable
Average Tensile (ksi.)	39.9	92.4	39.9	115.5
Shear (ksi)	5.64	55.4	5.64	69.3
Combined (ksi)	41.5	124.7	Not Required (Reference 1)	
Bearing (ksi) Allowable (ksi) (S _y of lid material)	30.9	43.3	Not Required (Reference 1)	

2.10.2.8.6 Minimum Engagement Length for Bolt and Flange

For a 1"- 8UNC – 2A bolt, the material is SA-540 GR. B24 CL.1, with

$$S_u = 165 \text{ ksi.}, \text{ and}$$

$$S_y = 150 \text{ ksi (at room temperature)}$$

The ram port cover threaded insert material (Helicoil #1185-16CN-2500) is constructed from type 304 stainless steel and has the following material properties.

$$S_u = 75 \text{ ksi.}, \text{ and}$$

$$S_y = 30 \text{ ksi (at room temperature)}$$

The minimum engagement length, L_e , for the bolt and flange is ([8], Page 1149),

$$L_e = \frac{2A_t}{3.1416K_{n \max} \left[\frac{1}{2} + .57735n(E_{s \min} - K_{n \max}) \right]}$$

Where,

A_t = tensile stress area = 0.606 in.²,

n = number of threads per inch = 8

$K_{n \max}$ = maximum minor diameter of internal threads = 0.890 in. ([8], p. 1287)

$E_{s \min}$ = minimum pitch diameter of external threads = 0.9100 in. ([8], p. 1287)

Substituting the values given above,

$$L_e = \frac{2(0.606)}{(3.1416)0.890 \left[\frac{1}{2} + .57735(8)(0.9100 - 0.890) \right]} = 0.732 \text{ in.}$$

$$J = \frac{A_s \times S_{ue}}{A_n \times S_{ui}} \cdot [8]$$

Where, S_{ue} is the tensile strength of external thread material, and S_{ui} is the tensile strength of internal thread material.

$$A_s = \text{shear area of external threads} = 3.1416 n L_e K_{n \max} [1/(2n) + .57735 (E_{s \min} - K_{n \max})]$$

$$A_n = \text{shear area of internal threads} = 3.1416 n L_e D_{s \min} [1/(2n) + .57735(D_{s \min} - E_{n \max})]$$

For the bolt / Helicoil insert connection:

$E_{n \max}$ = maximum pitch diameter of internal threads = 0.9276 in. ([8], p. 1287).

$D_{s \min}$ = minimum major diameter of external threads = 0.9830 in. ([8], p. 1287)

Therefore,

$$A_s = 3.1416(8)(0.732)(0.890)[1/(2 \times 8) + .57735 (0.9100 - 0.890)] = 1.212 \text{ in.}^2$$

$$A_n = 3.1416(8)(0.732)(0.9830)[1/(2 \times 8) + .57735 (0.9830 - 0.9276)] = 1.710 \text{ in.}^2$$

So,

$$J = \frac{1.212(165.0)}{1.710(75.0)} = 1.559$$

$$Q = L_e J = (0.732)(1.559) = 1.141 \text{ in.}$$

The actual minimum engagement length = 2.50 in. > 1.141 in. (limited by threaded insert length).

2.10.2.9 Conclusions

1. Bolt stresses meet the acceptance criteria of NUREG/CR-6007 "Stress Analysis of Closure Bolts for Shipping Casks".
2. A positive (compressive) load is maintained during normal and accident condition loads since bolt preload is higher than all applied loads.
3. If the NUHOMS[®]-MP197 cask lid bolts are replaced after every 85 round trip shipments, they will not fail due to fatigue during transport.
4. The bolt, insert, and flange thread engagement length is acceptable.
5. The ram port cover bolts are acceptable with respect to bolt stress, seal compression, and engagement length.

2.10.2.10 References

1. Stress Analysis of Closure Bolts for Shipping Cask, NUREG/CR-6007, 1992.
2. American Society of Mechanical Engineers, ASME Boiler and Pressure Vessel Code, Section II, Part D, 1998 with 1999 addenda.
3. American Society of Mechanical Engineers, ASME Boiler and Pressure Vessel Code Section III, Division 1, Subsection NB, 1998 with 1999 addenda.
4. Draft American Standard Design Basis for Resistance to Shock and Vibration of Radioactive Material Packages Greater than One Ton in Truck Transport, ANSI N14.23, 1980.
5. Shock and Vibration Environments for Large Shipping Containers on Rail Cars and Trucks, NUREG 766510, 1977.
6. Design Criteria for the Structural Analysis of Shipping Cask Containment Vessels, U. S. Nuclear Regulatory Commission, Regulatory Guide 7.6, Revision 1, March 1978.
7. American Society of Mechanical Engineers, ASME Boiler and Pressure Vessel Code Section III, Division 1, Appendix, 1998 with 1999 addenda.
8. Machinery Handbook, 21st Ed, Industrial Press, 1979.
9. Helicoil Catalog, Heli-Coil 8-Pitch Inserts, Bulletin 913B.
10. Baumeister, T., Marks, L. S., *Standard Handbook for Mechanical Engineers*, 7th Edition, McGraw-Hill, 1967.

Table 2.10.2-1
Design Parameters for Lid Bolt Analysis

- D_b Nominal diameter of closure bolt; 1.500 in.
- K Nut factor for empirical relation between the applied torque and achieved preload is 0.1 for neolube
- Q Applied torque for the preload (in.-lb.)
- D_{lb} Closure lid diameter at bolt circle, 72.31 in.
- D_{lg} Closure lid diameter at the seal (outer) = 69.873 in.
- E_c Young's modulus of cask wall material, 27.6×10^6 psi. @ 200° F. [2]
- E_l Young's modulus of lid material, 27.8×10^6 psi. @ 200° F. [2]
- N_b Total number of closure bolts, 48
- N_{ul} Poisson's ratio of closure lid, 0.305, ([10], p. 5-6).
- P_{ei} Inside pressure of cask, 50 psig.
- D_{lo} Closure lid diameter at outer edge, 74.68 in.
- P_{li} Pressure inside the closure lid, 50 psig.
- t_c Thickness of cask wall, 7.00 in.
- t_l Thickness of lid, 4.5, 4.0 in.
- l_b Thermal coefficient of expansion, bolt material, 6.7×10^{-6} in. in.⁻¹ °F⁻¹ at 200°F [2]
- l_c Thermal coefficient of expansion, cask, 8.5×10^{-6} in. in.⁻¹ °F⁻¹ at 200°F [2]
- l_l Thermal coefficient of expansion, lid, 5.90×10^{-6} in. in.⁻¹ °F⁻¹ at 200°F [2]
- E_b Young's modulus of bolt material, 27.1×10^6 psi. at 200°F [2]
- ai Maximum rigid-body impact acceleration (g) of the cask
- DLF Dynamic load factor to account for any difference between the rigid body acceleration and the acceleration of the contents and closure lid = 1.1
- W_c weight of contents = 43,005 lb. (fuel) + 22,918 lb. (basket) + 22,467 lb. (canister) = 88,390 lbs., conservatively use 90,000 lb. (Section 2.2)
- W_l weight of lid = 5,611 lbs., say 6,000 lbs.
- W_c+W_l 90,000 + 6,000 = 96,000 lbs.
- xi Impact angle between the cask axis and target surface
- S_{yl} Yield strength of closure lid material, 106.3 ksi. @ 200° F. [2]
- S_{ul} Ultimate strength of closure lid, 140,000 psi.
- S_{yb} Yield strength of bolt material (see Table 2.10.2-3).
- S_{ub} Ultimate strength of bolt material (see Table 2.10.2-4).
- P_{lo} Pressure outside the lid.
- L_b Bolt length between the top and bottom surfaces of closure, 2.27 in.
- P_{un} Maximum impact force that can be generated by the puncture bar during a normal impact.
- D_{pb} Puncture bar diameter, 6 inches as per 10 CFR 71.73 (c) (3).

Table 2.10.2-2

Bolt Data ([1], Table 5.1)

Lid Bolts:

Bolt: 1 1/2" - 6UNC - 2A

N : no of threads per inch = 6

p : Pitch = 1/6" = .167 in.

D_b : Nominal Diameter = 1.50 in.

D_{ba} : Bolt diameter for stress calculations = $D_b - .9743p = 1.50 - .9743 (.167) = 1.337$
in

Stress Area = $\pi/4 (1.337)^2 = 1.404 \text{ in}^2$

Ram Closure Bolts:

Bolt: 1" - 8UNC - 2A

N : no of threads per inch = 8

p : Pitch = 1/8" = .125 in.

D_b : Nominal Diameter = 1.00 in.

D_{ba} : Bolt diameter for stress calculations = $D_b - .9743p = 1.00 - .9743 (.125) = 0.878$ in

Stress Area = $\pi/4 (0.878)^2 = 0.606 \text{ in}^2$

Table 2.10.2-3

Allowable Stresses in Closure Bolts for Normal Conditions of Transport

(MATERIAL: SA-540 Gr. B24 CL.1)

Temperature (°F)	Yield Stress ⁽¹⁾ (ksi)	Normal Condition Allowables		
		F_{tb} ^(2,4) (ksi)	F_{vb} ^(3,4) (ksi)	$S.I.$ ⁽⁵⁾ (ksi)
100	150	100.0	60.0	135.0
200	143.4	95.6	57.4	129.1
300	138.6	92.4	55.4	124.7
400	134.4	89.6	53.8	121.0
500	130.2	86.8	52.1	117.2
600	124.2	82.8	49.7	111.8

Notes:

1. Yield stress values are from ASME Code, Section II, Table Y-1 [2]
2. Allowable Tensile stress, $F_{tb} = 2/3 S_y$ ([1], Table 6.1)
3. Allowable shear stress, $F_{vb} = 0.4 S_y$ ([1], Table 6.1)
4. Tension and shear stresses must be combined using the following interaction equation:

$$\frac{\sigma_{tb}^2}{F_{tb}^2} + \frac{\tau_{yb}^2}{F_{yb}^2} \leq 1.0 \quad [1]$$

5. Stress intensity from combined tensile, shear and residual torsion loads, $S.I. \leq 0.9 S_y$ ([1], Table 6.1)

Table 2.10.2-4

Allowable Stresses in Closure Bolts for Hypothetical Accident Conditions

(MATERIAL: SA-540 Gr. B24 Cl.1)

Temperature (°F)	Yield Stress ⁽¹⁾ (ksi)	Accident Condition Allowables		
		$0.6 S_y$ ⁽³⁾ (ksi)	F_{tb} ^(2,4) (ksi)	F_{vb} ^(3,4) (ksi)
100	150.0	90.0	115.5	69.3
200	143.4	86.0	115.5	69.3
300	138.6	83.2	115.5	69.3
400	134.4	80.6	115.5	69.3
500	130.2	78.1	115.5	69.3
600	124.2	74.5	115.5	69.3

Notes:

1. Yield and tensile stress values are from ASME Code, [2] Table Y-1, Note that S_u is 165 ksi at all temperatures of interest.
2. Allowable Tensile stress, $F_{tb} = \text{MINIMUM}(0.7 S_u, S_y)$, where $0.7 S_u = 0.7 (165) = 115.5$ ksi. ([1], Table 6.3)
3. Allowable shear stress, $F_{vb} = \text{MINIMUM}(0.42 S_u, 0.6 S_y)$, where $0.42 S_u = 0.42 (165.) = 69.3$ ksi. ([1], Table 6.3)
4. Tension and shear stresses must be combined using the following interaction equation:

$$\frac{\sigma_{tb}^2}{F_{tb}^2} + \frac{\tau_{yb}^2}{F_{yb}^2} \leq 1.0 \quad [1]$$

Table 2.10.2-5
Design Parameters for Ram Port Cover Bolt Analysis

- D_b Nominal diameter of closure bolt; 1.00 in.
- K Nut factor for empirical relation between the applied torque and achieved preload is 0.1 for neolube
- Q Applied torque for the preload (in.-lb.)
- D_{lb} Closure lid diameter at bolt circle, 22.00 in.
- D_{lg} Closure lid diameter at the seal (outer) = 20.02 in.
- E_c Young's modulus of cask flange material, 27.0×10^6 psi. @ 300° F.
- N_b Total number of closure bolts, 12
- N_{ul} Poisson's ratio of closure material, 0.305, (Ref. 6, p. 5-6).
- P_{ei} Inside pressure of cask, 50 psig.
- D_{lo} RAM Port Cover diameter at outer edge, 23.88 in.
- D_{li} Closure lid diameter at inner edge, 17.26 in.
- P_{li} Pressure inside the closure lid, 50 psig.
- t_l Thickness of lid, 2.5 in.
- l_b Thermal coefficient of expansion, bolt material, 6.9×10^{-6} in. in.⁻¹ °F⁻¹ at 300°F
- l_c Thermal coefficient of expansion, cask, 8.8×10^{-6} in. in.⁻¹ °F⁻¹ at 300°F
- l_l Thermal coefficient of expansion, cover, 8.8×10^{-6} in. in.⁻¹ °F⁻¹ at 300°F
- E_b Young's modulus of bolt material, 26.7×10^6 psi. at 300°F
- E_l Young's modulus of cover material, 27.0×10^6 psi. @ 300° F.
- S_{yl} Yield strength of cover material, 43.3 ksi. @ 300° F.
- S_{ul} Ultimate strength of cover, 94.2 ksi.
- S_{yb} Yield strength of bolt material (see Table 3).
- S_{ub} Ultimate strength of bolt material (see Table 4).
- P_{to} Pressure outside the lid, 0 psi.

NUHOMS®-MP197 TRANSPORT PACKAGING

CHAPTER 3

TABLE OF CONTENTS

	<u>Page</u>
3. THERMAL EVALUATION	
3.1 Discussion	3-1
3.2 Summary of Thermal Properties of Components	3-3
3.3 Technical Specifications for Components	3-9
3.4 Thermal Evaluation for Normal Conditions of Transport	3-10
3.4.1 Thermal Model	3-10
3.4.1.1 Cask Body Model	3-10
3.4.1.2 Basket Model	3-12
3.4.1.3 Decay Heat Load	3-13
3.4.1.4 Solar Heat Load	3-13
3.4.2 Maximum Temperatures	3-14
3.4.3 Maximum Accessible Surface Temperature in the Shade	3-14
3.4.4 Minimum Temperatures	3-14
3.4.5 Maximum Internal Pressure	3-14
3.4.6 Maximum Thermal Stresses	3-14
3.4.7 Evaluation of Package Performance for Normal Conditions	3-15
3.5 Thermal Evaluation for Accident Conditions	3-16
3.5.1 Fire Accident Evaluation	3-16
3.5.2 Cask Cross Section Model	3-16
3.5.3 Cask Body Model	3-17
3.5.4 Trunnion Region Model	3-17
3.5.5 Bearing Block Region Model	3-18
3.5.6 Maximum Internal Pressure	3-18
3.5.7 Summary of the Results	3-18
3.5.8 Evaluation of Package Performance during Fire Accident Conditions	3-19
3.6 References	3-20
3.7 Appendices	
3.7.1 Effective Thermal Conductivity for the Fuel Assembly	3.7.1-1
3.7.2 Average Heat Transfer Coefficient for Fire Accident Conditions	3.7.2-1
3.7.3 Maximum Internal Operating Pressures	3.7.3-1
3.7.4 Thermal Evaluation for Vacuum Drying Conditions	3.7.4-1

LIST OF TABLES

- 3-1 Component Temperatures in the NUHOMS[®]-MP197 Packaging
- 3-2 Temperature Distribution in the NUHOMS[®]-MP197 Package (Minimum Ambient Temperatures)
- 3-3 Maximum Transient Temperatures during Fire Accident

LIST OF FIGURES

- 3-1 Finite Element Plot, Cask Body Model
- 3-2 Finite Element Plot, Basket and Canister Model
- 3-3 Temperature Distribution, Cask Body Model (Normal Conditions of Transport)
- 3-4 Temperature Distribution, Basket and Canister Model (Normal Conditions of Transport)
- 3-5 Temperature Distribution, Basket (Normal Conditions of Transport)
- 3-6 Temperature Distribution, Fuel Assembly (Normal Conditions of Transport)
- 3-7 Finite Element Plot, Cask Cross Section Model
- 3-8 Temperature Distribution, Cask Body Model, End of Fire (Hypothetical Accident Conditions)
- 3-9 Temperature Distribution, Cask Cross Section Model, End of Fire (Hypothetical Accident Conditions)
- 3-10 Temperature Distribution, Fuel Assembly, Peak Temperatures (Hypothetical Accident Conditions)
- 3-11 Finite Element Plot, Trunnion Region Model
- 3-12 Temperature Distribution, Trunnion Region Model (Time = 4.7 Hours)
- 3-13 Finite Element Plot, Bearing Block Region Model
- 3-14 Temperature Distribution, Bearing Block Region Model (Time = 2.9 Hours)

CHAPTER 3

THERMAL EVALUATION

3.1 Discussion

The NUHOMS®-MP197 packaging is designed to passively reject decay heat under normal conditions of transport and hypothetical accident conditions while maintaining appropriate packaging temperatures and pressures within specified limits. Objectives of the thermal analyses performed for this evaluation include:

- limits to ensure components perform their intended safety functions;
- Determination of temperature distributions to support the calculation of thermal stresses;
- Determination of the cask and the DSC cavity gas pressures;
- Determination of the maximum fuel cladding temperature. Determination of maximum and minimum temperatures with respect to cask materials

To establish the heat removal capability, several thermal design criteria are established for the packaging. These are:

- Containment of radioactive material and gases is a major design requirement. Seal temperatures must be maintained within specified limits to satisfy the containment function during normal transport and hypothetical accident conditions. A maximum long-term seal temperature limit of 400 °F is set for the Fluorocarbon O-Rings [8] & [15].
- Maximum temperatures of the containment structural components must not adversely affect the containment function.
- To maintain the stability of the neutron shield resin during normal transport conditions, an allowable temperature range of -40 to 300 °F (-40 to 149 °C) is set for the neutron shield.
- In accordance with 10CFR71.43(g) the maximum temperature of accessible package surfaces in the shade is limited to 185 °F (85 °C).
- A maximum fuel cladding temperature limit of 570 °C (1058 °F) is set for the fuel assemblies with an inert cover gas [9].
- A maximum temperature limit of 327 °C (620 °F) is set for the lead, corresponding to the melting point [11].

The ambient temperature range for normal transport is -20 to 100°F (-29 to 38°C) per 10CFR71(b). In general, all the thermal criteria are associated with maximum temperature limits and not minimum temperatures. All materials can be subjected to a minimum environment temperature of -40°F (-40°C) without adverse effects, as required by 10CFR71(c)(2).

The NUHOMS[®]-MP197 is analyzed based on a maximum heat load of 15.86 kW from 61 fuel assemblies. The analyses consider the effect of the decay heat flux varying axially along a fuel assembly. The heat flux profile for a fuel assembly with a peak power factor of 1.2 and an active length of 144 in. is used for the evaluation. A description of the detailed analyses performed for normal transport conditions is provided in Section 3.4 and accident conditions in Section 3.5. A thermal analysis performed for vacuum drying conditions is described in Appendix 3.7.4. A summary of the analysis is provided in Table 3-1. The thermal evaluation concludes that with this design heat load, all design criteria are satisfied.

3.2 Summary of Thermal Properties of Materials

The analyses use interpolated values when appropriate for intermediate temperatures where the temperature dependency of a specific parameter is deemed significant. The interpolation assumes a linear relationship between the reported values.

1. BWR Fuel

Temperature (°F)	Thermal Conductivity (Btu/hr-in-°F)		Specific Heat (Btu/lbm-F)	Density (lbm/in ³)
	Transverse	Axial		
116.804	0.0137	0.0437	0.0574	0.105
214.424	0.0160
312.419	0.0186
410.726	0.0215
509.254	0.0249
608.009	0.0288	0.0437	0.0574	0.105

The fuel conductivity analysis, including determination of specific heat and density values, is presented in Appendix 3.7.1.

2. Helium

Temperature		Conductivity	
(K) [2]	(°F)	(W/m-K) [2]	(Btu/hr-in-°F)
100	-280	0.0073	0.0004
150	-190	0.0095	0.0005
200	-100	0.1151	0.0055
250	-10	0.1338	0.0064
300	80	0.1500	0.0072
400	260	0.1800	0.0087
500	440	0.2110	0.0102
600	620	0.2470	0.0119
800	980	0.3070	0.0148
1000	1340	0.3630	0.0175

3. Neutron Shielding (Polyester Resin)

Thermal Conductivity (Btu/hr-in-°F) [3]	Specific Heat (Btu/lbm-°F) [3]	Density (lbm/in ³) [3]
0.0087	0.3107	0.051

4. SA-240, Type 304 Stainless Steel

Temperature [1] (°F)	Thermal Conductivity [1] (Btu/hr-ft-°F)	Thermal Conductivity (Btu/hr-in-°F)	Diffusivity [1] (ft ² /hr)	Specific Heat (Btu/lbm-°F)	Density [1] (lbm/in ³)
70	8.6	0.717	0.151	0.117	0.282
100	8.7	0.725	0.152	0.117	...
150	9.0	0.750	0.154	0.120	...
200	9.3	0.775	0.156	0.122	...
250	9.6	0.800	0.158	0.125	...
300	9.8	0.817	0.160	0.126	...
350	10.1	0.842	0.162	0.128	...
400	10.4	0.867	0.165	0.129	...
450	10.6	0.883	0.167	0.130	...
500	10.9	0.908	0.170	0.131	...
550	11.1	0.925	0.172	0.132	...
600	11.3	0.942	0.174	0.133	...
650	11.6	0.967	0.177	0.134	...
700	11.8	0.983	0.179	0.135	...
750	12.0	1.000	0.181	0.136	...
800	12.2	1.017	0.184	0.136	...
850	12.5	1.042	0.186	0.138	...
900	12.7	1.058	0.189	0.138	...
950	12.9	1.075	0.191	0.138	...
1000	13.2	1.100	0.194	0.139	...
1050	13.4	1.117	0.196	0.140	...
1100	13.6	1.133	0.198	0.141	...
1150	13.8	1.150	0.201	0.141	...
1200	14.0	1.167	0.203	0.141	...
1250	14.3	1.192	0.205	0.143	...
1300	14.5	1.208	0.208	0.143	...
1350	14.7	1.225	0.210	0.143	...
1400	14.9	1.242	0.212	0.144	...
1450	15.1	1.258	0.214	0.145	...
1500	15.3	1.275	0.216	0.145	0.282

5. SA-36 Carbon Steel

Temperature [1] (°F)	Thermal Conductivity [1] (Btu/hr-ft-°F)	Thermal Conductivity (Btu/hr-in-°F)	Diffusivity [1] (ft ² /hr)	Specific Heat (Btu/lbm-°F)	Density [1] (lbm/in ³)
70	23.6	1.967	0.454	0.107	0.282
100	23.9	1.992	0.443	0.111	...
150	24.2	2.017	0.433	0.115	...
200	24.4	2.033	0.422	0.118	...
250	24.4	2.033	0.414	0.121	...
300	24.4	2.033	0.406	0.123	...
350	24.3	2.025	0.396	0.126	...
400	24.2	2.017	0.386	0.128	...
450	23.9	1.992	0.375	0.131	...
500	23.7	1.975	0.364	0.133	...
550	23.4	1.950	0.355	0.135	...
600	23.1	1.925	0.346	0.137	...
650	22.7	1.892	0.333	0.140	...
700	22.4	1.867	0.320	0.143	...
750	22.0	1.833	0.308	0.146	...
800	21.7	1.808	0.298	0.149	...
850	21.2	1.767	0.286	0.152	...
900	20.9	1.742	0.274	0.156	...
950	20.5	1.708	0.262	0.160	...
1000	20.0	1.667	0.248	0.165	...
1050	19.6	1.633	0.237	0.169	...
1100	19.2	1.600	0.228	0.173	...
1150	18.7	1.558	0.213	0.180	...
1200	18.2	1.517	0.197	0.189	...
1250	17.5	1.458	0.179	0.200	...
1300	16.7	1.392	0.155	0.221	...
1350	15.8	1.317	0.119	0.272	...
1400	15.3	1.275	0.077	0.407	...
1450	15.1	1.258	0.154	0.201	...
1500	15.1	1.258	0.169	0.183	0.282

6. SA-705, Type 630 Stainless Steel

Temperature [1] (°F)	Thermal Conductivity [1] (Btu/hr-ft-°F)	Thermal Conductivity (Btu/hr-in-°F)	Diffusivity [1] (ft ² /hr)	Specific Heat (Btu/lbm-°F)	Density [1] (lbm/in ³)
70	9.9	0.825	0.188	0.108	0.282
100	10.1	0.842	0.189	0.110	...
150	10.4	0.867	0.189	0.113	...
200	10.6	0.883	0.189	0.115	...
250	10.9	0.908	0.190	0.118	...
300	11.2	0.933	0.190	0.121	...
350	11.4	0.950	0.191	0.122	...
400	11.7	0.975	0.191	0.126	...
450	12.0	1.000	0.191	0.129	...
500	12.2	1.017	0.190	0.132	...
550	12.5	1.042	0.190	0.135	...
600	12.7	1.058	0.190	0.137	...
650	13.0	1.083	0.188	0.142	...
700	13.2	1.100	0.186	0.145	...
750	13.4	1.117	0.183	0.150	...
800	13.5	1.125	0.180	0.154	...
850	13.6	1.133	0.176	0.158	...
900	13.7	1.142	0.172	0.163	...
950	13.8	1.150	0.167	0.169	...
1000	13.8	1.150	0.160	0.177	...
1050	13.9	1.158	0.153	0.186	...
1100	14.0	1.167	0.146	0.196	...
1150	14.1	1.175	0.134	0.216	...
1200	14.2	1.183	0.129	0.226	...
1250	14.4	1.200	0.140	0.211	...
1300	14.6	1.217	0.152	0.197	...
1350	14.8	1.233	0.171	0.177	...
1400	15.0	1.250	0.185	0.166	...
1450	15.2	1.267	0.194	0.161	...
1500	15.4	1.283	0.201	0.157	0.282

7. Air

Temperature		ν [2]	μ [2]	Pr [2]	Conductivity		Kin. Visc.
(K) [2]	(°F)	(m ² /kg)	(Pa-s)	(---)	(W/m-K) ⁽²⁾	(Btu/hr-ft-°F)	(ft ² /s)
200	-100	0.573	1.33E-5	0.740	0.0181	0.0105	8.203E-05
300	80	0.861	1.85E-5	0.708	0.0263	0.0152	1.715E-04
400	260	1.148	2.30E-5	0.694	0.0336	0.0194	2.842E-04
500	440	1.436	2.70E-5	0.688	0.0404	0.0233	4.173E-04
600	620	1.723	3.06E-5	0.690	0.0466	0.0269	5.675E-04
800	980	2.298	3.70E-5	0.705	0.0577	0.0333	9.152E-04
1000	1340	2.872	4.24E-5	0.707	0.0681	0.0393	1.311E-03

8. Wood

Thermal Conductivity ⁽ⁱ⁾ (Btu/hr-in-°F)	
Min.	Max.
0.0019	0.0378

(i) bounds, perpendicular to and parallel to the grain, wood conductivities in both References 4 and 5 for moisture contents up to 30% and specific gravities between 0.08 and 0.80. The bounding minimum conductivity is used during normal conditions and during the pre- and post-fire accident condition. The maximum wood conductivity is used during the fire accident condition.

(ii) wood is conservatively given no thermal mass ($\rho=0$, $C_p = 0$)

9. Poison Plates

Specific Heat	Density
Btu/lbm-°F	lbm/in ³
0.214	0.098

Properties are from Reference 2 for aluminum. The thermal conductivities are specified in Section 3.3 for the neutron poison plates and will be verified via testing.

10. Aluminum Alloy 6063-T5

Temperature [1] (°F)	Thermal Conductivity [1] (Btu/hr-ft-°F)	Thermal Conductivity (Btu/hr-in-°F)	Diffusivity [1] (ft ² /hr)	Specific Heat (Btu/lbm-°F)	Density [1] (lbm/in ³)
70	120.8	10.067	3.34	0.216	0.097
100	120.3	10.025	3.30	0.217	...
150	119.7	9.975	3.23	0.221	...
200	119.1	9.925	3.18	0.223	...
250	118.3	9.858	3.13	0.225	...
300	118.3	9.858	3.09	0.228	...
350	117.9	9.825	3.04	0.231	...
400	117.6	9.800	3.00	0.234	0.097

11. Lead

Temperature		Conductivity		Specific Heat		Density	
(K) [2]	(°F)	(W/m-K) [2]	(Btu/hr-in-°F)	(kJ/kg-K) [2]	(Btu/lbm-°F)	(kg/m ³) [2]	(lbm/in ³)
200	-100	36.7	1.767	0.125	0.030	11,330*	0.409
250	-10	36.0	1.733	0.127	0.030
300	80	35.3	1.700	0.129	0.031
400	260	34.0	1.637	0.132	0.032
500	440	32.8	1.579	0.137	0.033
600	620	31.4	1.512	0.142	0.034	11,330*	0.409

12. Emissivities and Absorptivities

Thermal radiation effects at the external surfaces of the packaging are considered. Impact limiter external surfaces are painted white. The emissivity of white paint varies between 0.93-0.95 and the solar absorptivity varies between 0.12-0.18 ([2] & [6]). To account for dust and dirt, the thermal analysis uses a solar absorptivity of 0.30 and an emissivity of 0.90 for the exterior surfaces of the impact limiters.

The external surface of the cask body is weathered stainless steel (emissivity = 0.85, [6]). To account for dust and dirt and to bound the problem, the thermal analysis uses a solar absorptivity of 0.9 and an emissivity of 0.8 for the cask body external surface.

After a fire, the cask surface will be partially covered in soot (emissivity = 0.95, [7]). Painted surfaces are given a post-fire emissivity of 0.90. The cask body surfaces are given a post-fire emissivity of 0.80. To bound the problem all surfaces are given a solar absorptivity of unity after the fire accident condition.

3.3 Technical Specifications for Components

The neutron poison plates will have the following minimum conductivity:

Temperature		Conductivity	
(°C)	(°F)	(W/m-°C)	(Btu/hr-in-°F)
20	68	120	5.78
100	212	145	6.98
250	482	150	7.22
300	571	150	7.22

3.4 Thermal Evaluation for Normal Conditions of Transport

The normal conditions of transport are used for determination of the maximum fuel cladding temperature, NUHOMS®-MP197 component temperatures, confinement pressures and thermal stresses. These steady state environmental conditions correspond to the maximum daily averaged ambient temperature of 100 °F and the 10CFR Part 71.71(c) insolation averaged over a 24 hour period.

3.4.1 Thermal Models

The finite element models are developed using the ANSYS computer code [10]. ANSYS is a comprehensive thermal, structural, and fluid flow analysis package. It is a finite element analysis code capable of solving steady-state and transient thermal analysis problems in one, two, and three dimensions. Heat transfer via a combination of conduction, radiation, and convection can be modeled by ANSYS. The three-dimensional geometry of the packaging was modeled. Solid entities were modeled by SOLID70 three-dimensional thermal elements. SURF152 surface effect elements were used for the application of the solar heat load.

Two finite element models are used for the normal conditions of transport evaluation:

- A cask body model to determine temperature distributions within the cask body, impact limiters, and thermal shield.
- A basket model to determine temperature distributions within the DSC and it's contents. This model also includes the helium gap between the DSC and the cask cavity inner surfaces.

The interior nodes of the cask body model line up with the exterior nodes of the basket model. The analysis is performed by first running the cask body model. The temperatures on the inner cavity surfaces are then applied as a boundary condition to the exterior nodes of the basket model. This approach allowed the modeling of sufficient detail within the packaging while keeping the overall size of the individual models reasonable.

3.4.1.1 Cask Body Model

To determine component temperatures within the cask body during normal conditions of transport, a finite element model of the cask body is developed. The three-dimensional model represents a 90° symmetric section of the packaging and includes the geometry and material properties of the impact limiters, thermal shield, the cask body, lead, neutron shielding (resin in aluminum containers), and outer shell.

The neutron shielding consists of 60 long slender resin-filled aluminum containers placed between the cask body and outer stainless steel shell. The aluminum containers are confined between the cask body and outer shell, and butt against the adjacent shells. For conservatism, an air gap of 0.01 in. at thermal equilibrium is assumed to be present between the resin boxes and adjacent shells. Radiation across these gaps is conservatively neglected. The redwood and balsa

within the impact limiters are modeled as a homogenized region containing bounding material properties.

The finite element plot of the cask body model is shown in Figure 3-1.

Generally, good surface contact is expected between adjacent components. However, to bound the heat conductance uncertainty between adjacent components, the following gaps at thermal equilibrium are assumed:

- 0.0100" radial gaps between resin boxes and adjacent shells
- 0.0300" radial gap between lead and cask body
- 0.0600" radial gap between cask lid and cask body
- 0.0625" axial gap between cask lid and cask body
- 0.0600" radial and axial gaps between ram plate and cask body
- 0.0625" axial gap between rear impact limiter and thermal shield
- 0.0625" axial gap between thermal shield and cask body
- 0.1250" axial gap between front impact limiter and cask body
- 0.0625" axial gap between thermal shield and impact limiter

All heat transfer across the gaps is by gaseous conduction. Other modes of heat transfer are neglected.

Heat Dissipation

Heat is dissipated from the surface of the packaging by a combination of radiation and natural convection.

Heat dissipation by natural convection is described by the following equations for the average Nusselt number [11]:

$$\bar{N}_{ul} = \bar{H}_c \frac{L}{k} = 0.13(G_{rL} Pr)^{1/3} \quad \text{for } Pr G_{rL} > 10^9 \quad (\text{Horizontal cylinders and vertical surfaces})$$

$$\bar{N}_{ul} = \bar{H}_c \frac{L}{k} = 0.59(G_{rL} Pr)^{1/4} \quad \text{for } 10^4 < Pr G_{rL} < 10^9 \quad (\text{vertical surfaces})$$

where,

- G_{rL} = Grashof number = $\rho^2 g \beta (T_s - T_a) L^3 / \mu^2$
- ρ = density, lb/ft³
- g = acceleration due to gravity, ft/sec²
- β = temperature coefficient of volume expansion, 1/R
- μ = absolute viscosity, lb/ft-sec
- L = characteristic length, ft
- Pr = Prandtl number
- H_c = natural convection coefficient

The heat transfer coefficient, H_r , for heat dissipation by radiation, is given by the equation:

$$H_r = G_{12} \left[\frac{\sigma(T_1^4 - T_2^4)}{T_1 - T_2} \right] \text{Btu/hr} \cdot \text{ft}^2 \cdot ^\circ\text{F}$$

where,

- G_{12} = the gray body exchange coefficient
= (surface emissivity) (view factor)
- T_1 = ambient temperature, $^\circ\text{R}$
- T_2 = surface temperature, $^\circ\text{R}$

The total heat transfer coefficient $H_t = H_r + H_c$, is applied as a boundary condition on the outer surfaces of the finite element model.

3.4.1.2 Basket Model

To determine component temperatures within the canister and its contents during normal conditions of transport a finite element model is developed. The three-dimensional model represents a 90° symmetric section of the packaging and includes the geometry and material properties of the canister, basket, fuel assembly active lengths, basket peripheral inserts, and the helium between the canister and the cask body.

The finite element plot of the basket model is shown in Figure 3-2.

To bound the heat conductance uncertainty between adjacent packaging components the following gaps at thermal equilibrium are assumed:

- 0.0100" surrounding outside of the fuel compartments
- 0.0100" between the fuel compartment wrap and plates parallel to the wrap
- 0.0400" between the fuel compartment wrap and plates perpendicular to the wrap
- 0.0950" between perpendicular plates
- 0.0100" between plates and basket rails
- 0.1250" axial gap between bottom of canister and cask body

Maximum Fuel Cladding Temperature

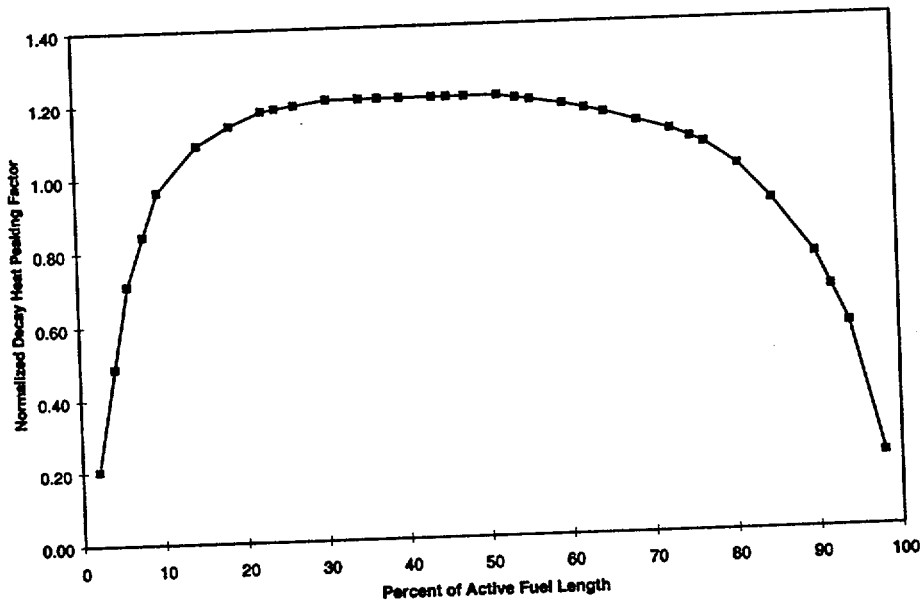
The finite element model includes a representation of the spent nuclear fuel that is based on a fuel effective conductivity model. The decay heat of the fuel with a peaking factor of 1.2 was applied directly to the fuel elements. The maximum fuel temperature reported is based on the results of the temperature distribution in the fuel region of the model. As described in Appendix 3.7.1, the homogenized fuel properties are chosen to match both the temperature drop between basket walls and fuel assembly center pin, and the effective conductivity of the fuel assemblies.

Average Cavity Gas Temperature

The cavity gas temperatures are calculated using maximum component temperatures under normal and hypothetical accident conditions of transport. For simplicity and conservatism, the average gas temperature within the canister is assumed to be the average of the maximum fuel cladding and canister wall temperatures. Within the cask body the average cavity gas temperature is taken to be the average of the maximum cask body and canister wall temperatures.

3.4.1.3 Decay Heat Load

The decay heat load corresponds to a total heat load of 15.86 kW from 61 assemblies (0.260 kW/assy.) with a peaking factor of 1.2. A typical heat flux profile for spent BWR fuel with an axial peaking factor of 1.2 was used to distribute the decay heat load in the axial direction within the active length regions of the models. This heat flux profile is shown below. Within the basket model, the decay heat load is applied as volumetric heat generation in the elements that represent the homogenized fuel. Within the Cask Body model the heat is applied as heat fluxes into the elements that model the cask cavity wall.



3.4.1.4 Solar Heat Load

The total insolation for a 12-hour period in a day is 1475 Btu/ft² for curved surfaces and 738 Btu/ft² for flat surfaces not transported horizontally as per 10CFR Part 71.71(c). This insolation is averaged over a 24-hr period (daily averaged value) and applied as a constant steady state value to the external surfaces of the cask body model. Solar absorptivities of 0.30 and 0.9 are used for the painted and stainless steel surfaces of the packaging, respectively. Daily averaging of the solar heat load is justified based on the large thermal inertia of the NUHOMS[®]-MP197 packaging.

3.4.2 Maximum Temperatures

Steady state thermal analyses are performed using the maximum decay heat load of 0.260 kW per assembly (15.86 kW total), 100°F ambient temperature and the maximum insolation. The temperature distributions within the cask body and basket models are shown in Figures 3-3 and 3-4, respectively. The temperature distribution within the basket is shown in Figure 3-5. The fuel assembly temperature distribution is shown in Figure 3-6. A summary of the calculated cask component temperatures is listed in Table 3-1.

3.4.3 Maximum Accessible Surface Temperature in the Shade

The accessible surfaces of the NUHOMS[®]-MP197 packaging consist of the personnel barrier and outermost vertical and radial surfaces of the impact limiters. The cask body model is run without insolation to determine the accessible surface temperature of the impact limiters in the shade. The maximum accessible surface temperature of the impact limiters in the shade does not exceed 110 °F.

The personnel barrier surrounds approximately one fourth of the cask body and has an open area of at least 80%. Heat transfer between the cask and barrier will be minimal due to the small radiation view factor between the cask and barrier. The personnel barrier rises 90 in. above the base of the transport frame and limits the accessible packaging surfaces to only the impact limiter surfaces. Accessible surfaces of the packaging remain below the design criteria of 185 °F (85 °C).

3.4.4 Minimum Temperatures

Under the minimum temperature condition of -40°F (-40°C) ambient, the resulting packaging component temperatures will approach -40°F if no credit is taken for the decay heat load. Since the package materials, including containment structures and the seals, continue to function at this temperature, the minimum temperature condition has no adverse effect on the performance of the NUHOMS[®]-MP197.

Temperature distributions under the minimum ambient temperatures of -20°F and -40°F with no insolation and the maximum design heat load are determined. Table 3-2 lists the results of these analyses.

3.4.5 Maximum Internal Operating Pressure

The maximum internal pressures within the NUHOMS[®]-MP197 cask body and DSC during normal conditions of transport are calculated within Appendix 3.7.3.

3.4.6 Maximum Thermal Stresses

The maximum thermal stresses during normal conditions of transport are calculated in Chapter 2.

3.4.7 Evaluation of Cask Performance for Normal Conditions of Transport

The thermal analysis for normal transport concludes that the NUHOMS®-MP197 packaging design meets all applicable requirements. The maximum component temperatures calculated using conservative assumptions are low. The maximum seal temperature (217°F, 103°C) during normal transport is well below the 400°F long-term limit specified for continued seal function. The maximum neutron shield temperature is below 300°F (149°C) and no degradation of the neutron shielding is expected. The predicted maximum fuel cladding temperature is well within allowable fuel temperature limit of 1058°F (570°C). The comparison of the results with the allowable ranges is tabulated below:

Component	Temperature, °F		
	Maximum	Minimum	Allowable Range
Seal	217	-40	-40 to 400
Neutron Shield	249	-40	-40 to 300
Fuel Cladding	598	-40	1058 max.
Lead	299	-40	620 max.

3.5 Thermal Evaluation for Accident Conditions

The NUHOMS[®]-MP197 packaging is evaluated under the hypothetical accident sequence of 10CFR71.73. In order to demonstrate that the seal, fuel cladding, and lead temperatures remain below thermal design requirements, four analytical models are developed as discussed below.

3.5.1 Fire Accident Evaluation

The fire thermal evaluation is performed primarily to demonstrate the containment integrity of the packaging. This is assured as long as the containment seals remain below 400°F and the cavity pressure is less than 50 psig (4.4 atm absolute pressure). Four models are used for the evaluation:

- A cask cross-section model for the determination of the peak fuel cladding temperature.
- A cask body model to evaluate the performance of the seals under hypothetical accident conditions.
- A trunnion-region model to demonstrate that lead remains below its melting point during hypothetical accident conditions.
- A bearing block-region model to demonstrate that lead remains below its melting point during hypothetical accident conditions.

During the free drop and puncture conditions, the steel encased wood impact limiters are locally deformed but remain firmly attached to the cask. Because of the very low conductivity of wood, a minimal amount of wood is required to provide adequate insulation during the fire accident condition. Therefore, there is a negligible change in the thermal performance of the impact limiters due to dimensional changes caused by the hypothetical accident conditions of 10CFR71.73. Under exposure to the thermal accident environment the wood at the periphery of the impact limiter shell would char but not burn.

An average convective heat transfer coefficient of 2.75 Btu/hr-ft²-°F is utilized for the fire accident evaluation as calculated in Appendix 3.7.2.

3.5.2 Cask Cross Section Model

To demonstrate that the peak fuel cladding temperature remains below thermal design limits, a cask cross-section finite element model of the NUHOMS[®]-MP197 packaging was developed. The three-dimensions, quarter-symmetry model includes the cask body, canister, basket, and fuel along the 144" active fuel length. To bound the heat conductance uncertainty between adjacent packaging components the same gap assumptions made in sections 3.4.1.1 and 3.4.1.2 are applied to the model.

During the pre-fire condition, convection and radiation from the external surface of this model are as in normal conditions of transport (100°F ambient). During the fire phase, a constant convective heat transfer coefficient of 2.75 Btu/hr-ft²-°F is used. As per 10CFR71.73, a 30 minute 1,475°F flame temperature with an emittance of 0.9 and a surface absorptivity of 0.8 is used during the fire accident condition. During the fire accident condition, gaps within the cask body and basket were removed to maximize heat input into the model from the fire. These gaps are included during the pre- and post-fire accident conditions. See Section 3.4.1 for a detailed description of the model including the method used to calculate the maximum fuel cladding temperature and the average cavity gas temperature. The decay heat load is applied as per Section 3.4.1.3.

The Cask Cross Section finite element model and the temperature distribution at the end of the fire accident condition are shown in Figures 3-7 and 3-9, respectively. The maximum temperature distribution within the fuel assemblies is shown in Figure 3-10.

3.5.3 Cask Body Model

To demonstrate the integrity of the seals during the fire accident, the cask body finite element model of the NUHOMS[®]-MP197 packaging developed in Section 3.4.1.1 was run under hypothetical accident conditions. Pre-Fire, Fire accident, and Post-Fire cool-down boundary conditions are determined as per Section 3.5.2. During the fire accident condition, gaps within the packaging were removed to maximize heat input into the model from the fire. These gaps are included during the pre- and post-fire accident conditions. The decay heat load is applied as per Section 3.4.1.3.

The Cask Body finite element model and the temperature distribution at the end of the fire accident condition are shown in Figures 3-1 and 3-8, respectively.

3.5.4 Trunnion Region Model

To determine the peak transient lead temperature in the region of the trunnions, a trunnion region finite element model was developed. The two-dimensional, axisymmetric model represents the geometry and material properties of the trunnion block, trunnion plug, and cask body in the region of the trunnion.

To bound the heat conductance uncertainty between adjacent packaging components the following gaps at thermal equilibrium are assumed:

- 0.0100" between the trunnion plug and the neutron absorbing resin
- 0.0100" between the trunnion plug and the trunnion block
- 0.0100" between the resin and the cask outer shell
- 0.0100" between the trunnion block and the cask outer shell
- 0.0300" radial gap between lead and cask body

Pre-Fire, Fire accident, and Post-Fire cool-down boundary conditions are determined as per Section 3.5.2. During the fire accident condition, gaps within the packaging were removed to

maximize heat input into the model from the fire. These gaps are included during the pre- and post-fire accident conditions. The decay heat load is applied as a flux including a peaking factor of 1.2.

The trunnion region finite element model and the temperature distribution at the time of peak lead temperature are shown in Figures 3-11 and 3-12, respectively.

3.5.5 Bearing Block Region Model

To determine the peak transient lead temperature in the region of the bearing block, a bearing block region finite element model was developed. A three-dimensional quarter-symmetry finite element model was created of the bearing block including the geometry and material properties of the adjacent neutron shielding and the corresponding portion of the cask body. Solid entities were modeled by SOLID70 three-dimensional thermal elements.

To bound the heat conductance uncertainty between adjacent packaging components the following gaps at thermal equilibrium are assumed:

- 0.0100" radial gaps between resin boxes and adjacent shells
- 0.0300" radial gap between lead and cask body
- 0.0600" gap between the bearing block and the resin/resin boxes in radial, axial, and circumferential directions

Pre-Fire, Fire accident, and Post-Fire cool-down boundary conditions are determined as per Section 3.5.2. During the fire accident condition, gaps within the packaging were removed to maximize heat input into the model from the fire. These gaps are included during the pre- and post-fire accident conditions. The decay heat load is applied as a flux including a peaking factor of 1.2.

The bearing block region finite element model and the temperature distribution at the time of peak lead temperature are shown in Figures 3-13 and 3-14, respectively.

3.5.6 Maximum Internal Operating Pressure

The maximum internal pressures within the NUHOMS[®]-MP197 cask body and DSC during hypothetical accident conditions of transport are calculated within Appendix 3.7.3.

3.5.7 Summary of Results

Table 3-3 presents the maximum temperatures of the cask components during the fire event. The maximum temperatures calculated for the seals and the fuel cladding are 279°F and 680°F, respectively.

3.5.8 Evaluation of Package Performance during Fire Accident Conditions

It is concluded that the NUHOMS[®]-MP197 packaging maintains containment during the postulated accident conditions. The maximum seal temperature is below the 400°F limit specified for seal function and the fuel cladding temperature is well below the limit of 1058°F (570°C).

A comparison of the results with the temperature limits is tabulated below:

Component	Temperature, °F	
	Maximum	Limit
Seal	279	400 max.
Fuel Cladding	680	1058 max.
Lead	478	620 max.

3.6 References

1. *ASME Boiler and Pressure Vessel Code*, American Society of Mechanical Engineers, Section II, 1998.
2. *Handbook of Heat Transfer Fundamentals*, W. Rohsenow and J. Harnett, McGraw-Hill Publishing, New York, 1985.
3. *TN-24 Dry Storage Cask Topical Report*, Transnuclear, Inc., Revision 2A, Hawthorne, NY, 1989.
4. *Wood Handbook: Wood as an Engineering Material*, U.S. Department of Agriculture, Forest Service, March 1999.
5. NUREG/CR-0200, Vol. 3, Rev. 6, SCALE, A Modular Code System for Performing Standardized Computer Analyses for Licensing Evaluation.
6. *Principles of Heat Transfer, Fourth Edition*, Kreith et. al., Harper & Row, Publishers, New York, 1986.
7. *Standard Handbook for Mechanical Engineers, Seventh Edition*, Baumeister & Marks, McGraw-Hill Book Co., New York, 1969
8. *Parker O-Ring Handbook 5700*, Y2000 Edition, 1999
9. PNL-4835, Johnson et. al., Technical Basic for Storage of Zircalloy-Clad Spent Fuel in Inert Gases, Pacific Northwest Laboratory, 1983.
10. ANSYS Engineering Analysis System, *User's Manual for ANSYS Revision 5.6*, ANSYS, Inc., Houston, PA.
11. *Chemical Engineers' Handbook, Fifth Edition*, Perry P.H. and Chilton C.H., McGraw-Hill Book Co., New York, 1973.
12. *TN-68 Dry Storage Cask Final Safety Analysis Report*, Transnuclear Inc., Revision 0, Hawthorne, NY, 2000.
13. *Standard Review Plan for Transportation Packages for Spent Nuclear Fuel*, NUREG-1617, 2000.
14. NUHOMS COC 1004 Amendment No. 3, 2000
15. Material Report Number KJ0835, Parker O-Ring Division, 1989.

TABLE 3-1

COMPONENT TEMPERATURES IN THE NUHOMS®-MP197 PACKAGING

Component	Normal Transport			Fire Accident	
	Maximum (°F)	Minimum* (°F)	Allowable Range(°F)	Peak(°F)	Allowable Range(°F)
Thermal Shield	186	-40	**	1172	**
Impact Limiters	195	-40	**	N/A	N/A
Resin	249	-40	-40 to 300	N/A	N/A
Lead	299	-40	620 max.	478	620 max.
Cask Body	302	-40	**	535	**
Outer Shell	263	-40	**	N/A	**
Flouorocarbon Seals, Ram Plate	217	-40	-40 to 400	270	-40 to 400
Flouorocarbon Seals, Lid	204	-40	-40 to 400	279	-40 to 400
Canister	388	-40	**	485	**
Basket Peripheral Inserts	482	-40	**	564	**
Basket	578	-40	**	661	**
Fuel Cladding	598	-40	1058 max.	680	1058 max.
Average Cavity Gas (Cask Body)	345	-40	N/A	504	N/A
Average Cavity Gas (Canister)	493	-40	N/A	583	N/A

* Assuming no credit for decay heat and an ambient temperature of -40°F

** The components perform their intended safety function within the operating range.

TABLE 3-2

TEMPERATURE DISTRIBUTION IN THE NUHOMS®-MP197 PACKAGE
(MINIMUM AMBIENT TEMPERATURES)

<u>Component</u>	<u>Maximum Component Temperature</u>	
	<u>-20 °F Ambient</u>	<u>-40 °F Ambient</u>
Thermal Shield	65	47
Impact Limiters	73	56
Resin	128	111
Lead	183	167
Cask Body	187	170
Flourocarbon Seals, Ram Plate	187*	170*
Flourocarbon Seals, Lid	187*	170*
Canister	282	267
Basket Peripheral Inserts	381	367
Basket	482	468
Fuel Cladding	505	492

* Taken to be the maximum temperature within cask body and lid.

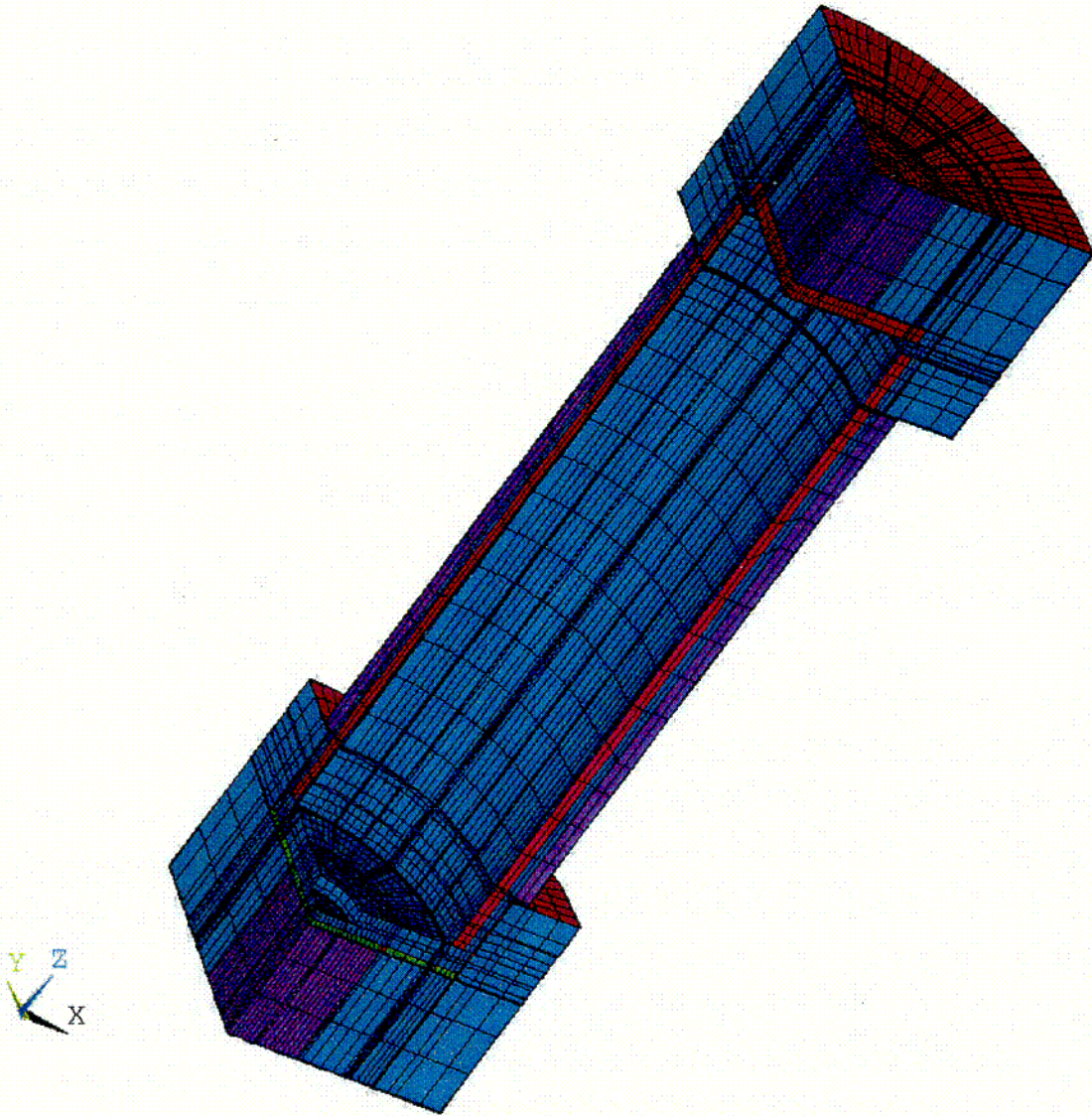
TABLE 3-3

MAXIMUM TRANSIENT TEMPERATURES DURING FIRE ACCIDENT

<u>Component</u>	<u>Maximum Transient</u>
Thermal Shield	1172 (End of Fire)
Lead	478 (4.7 Hours)
Cask Body	535 (End of Fire)
Flourocarbon Seals, Ram Plate	270 (31.0 Hours)
Flourocarbon Seals, Lid	279 (12.0 Hours)
Canister	485 (4.9 Hours)
Basket Peripheral Inserts	564 (15.9 Hours)
Basket	661 (24.9 Hours)
Fuel Cladding	680 (27.9 Hours)
Average Cavity Gas (Cask Body)	504
Average Cavity Gas (Canister)	583

FIGURE 3-1

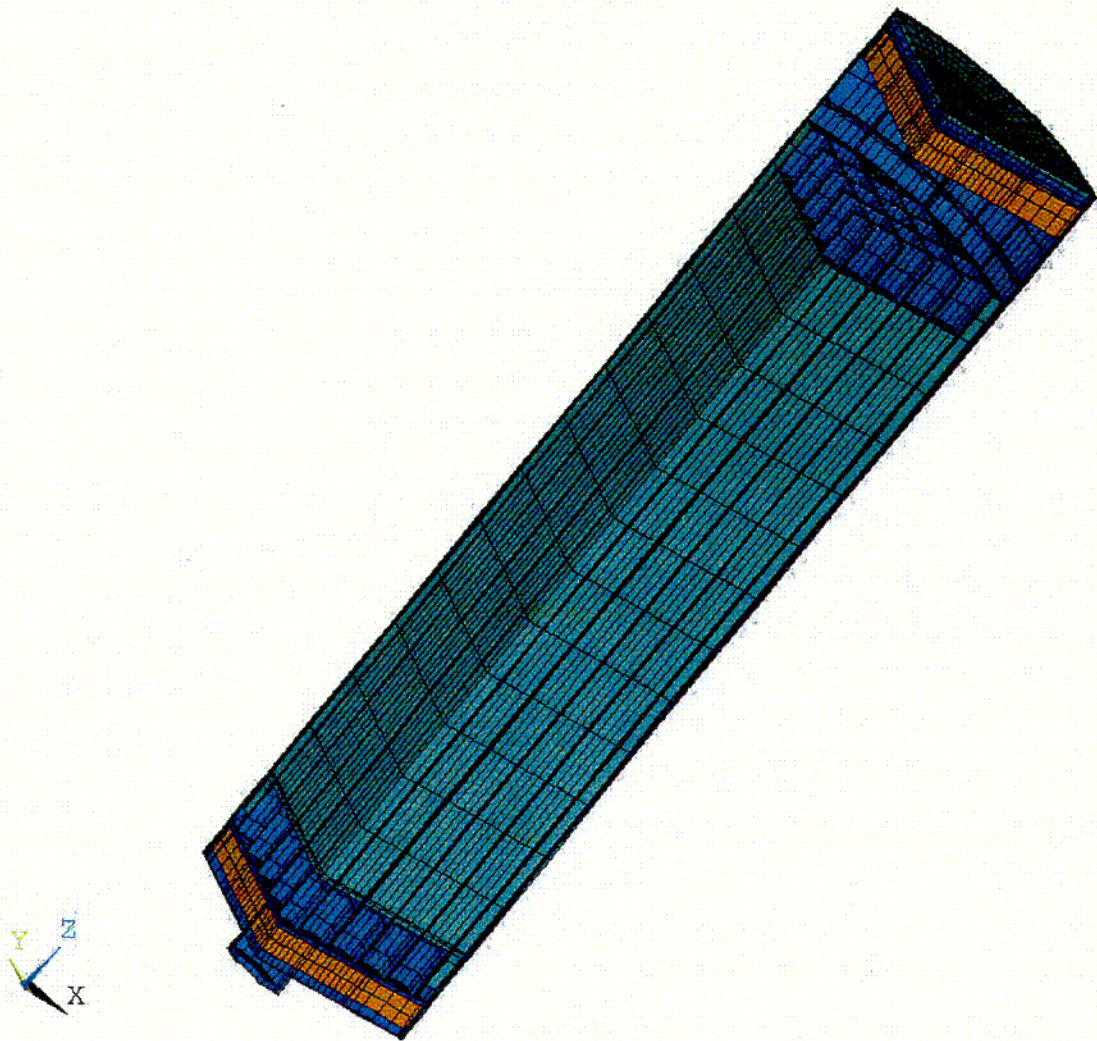
FINITE ELEMENT PLOT,
CASK BODY MODEL



C01

FIGURE 3-2

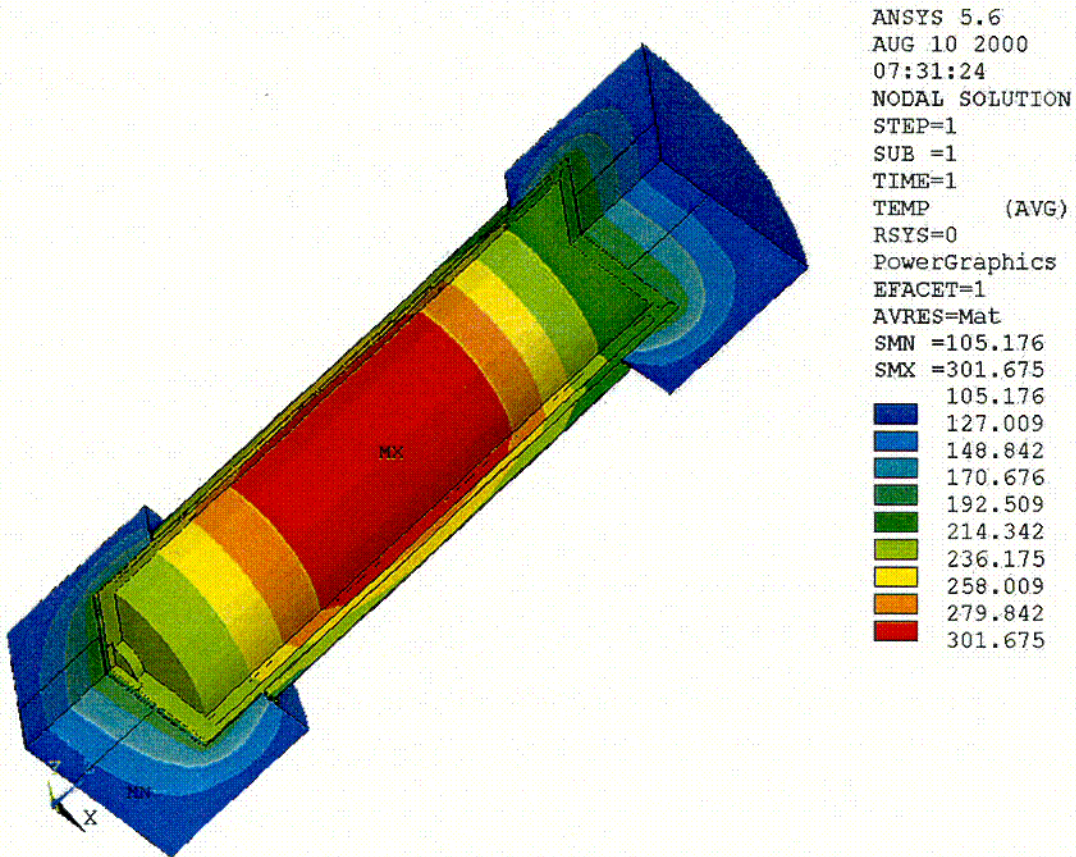
FINITE ELEMENT PLOT,
BASKET AND CANISTER MODEL



C02

FIGURE 3-3

TEMPERATURE DISTRIBUTION,
CASK BODY MODEL
(NORMAL CONDITIONS OF TRANSPORT)

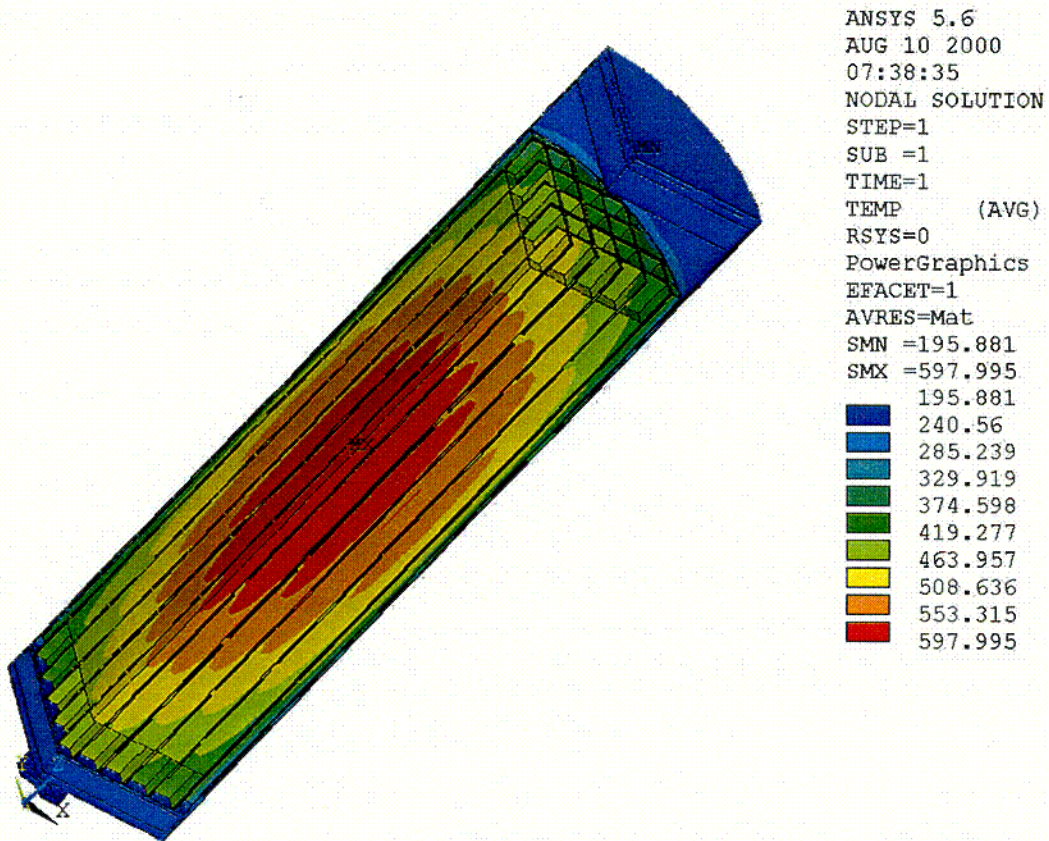


C03

Rev. 0 4/01

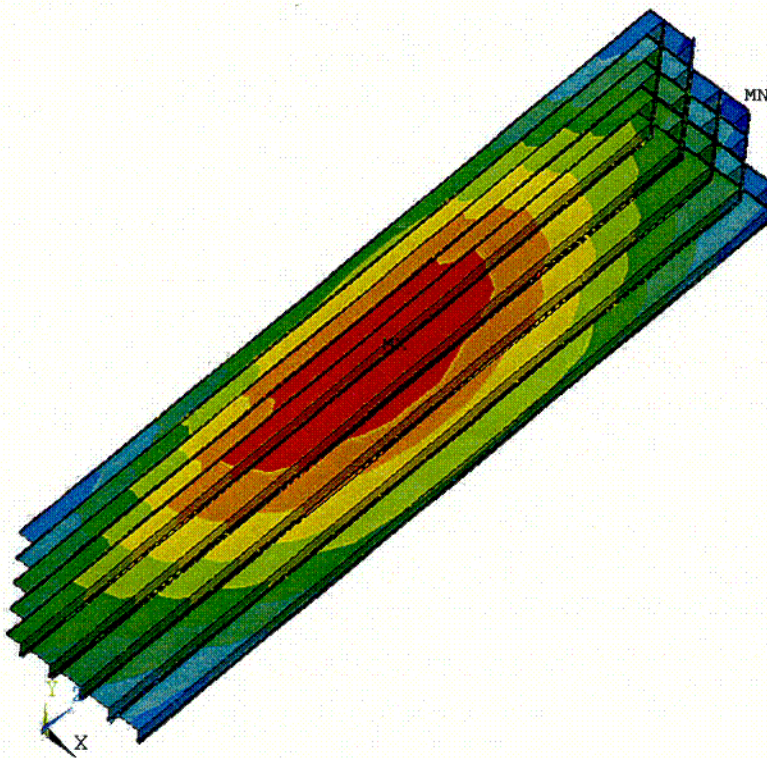
FIGURE 3-4

TEMPERATURE DISTRIBUTION,
BASKET AND CANISTER MODEL
(NORMAL CONDITIONS OF TRANSPORT)



C04

FIGURE 3-5
TEMPERATURE DISTRIBUTION,
BASKET
(NORMAL CONDITIONS OF TRANSPORT)

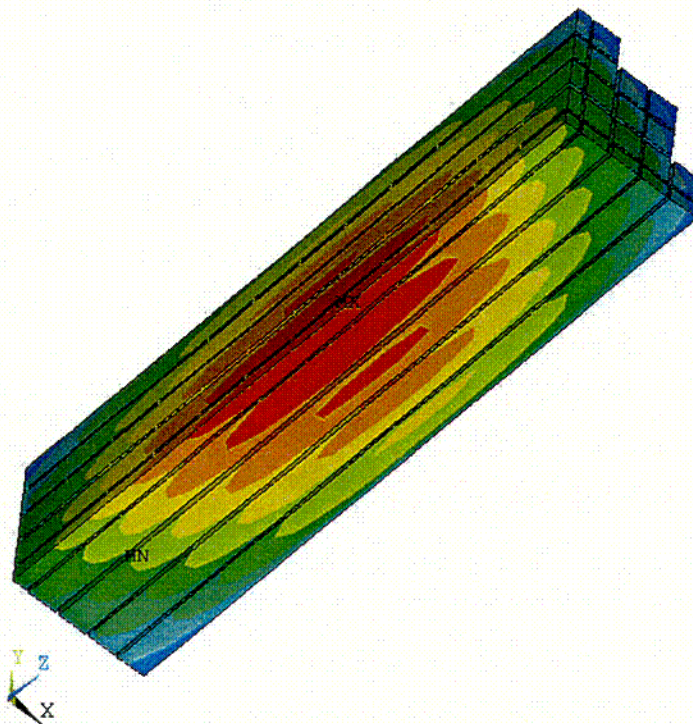


ANSYS 5.6
AUG 10 2000
07:41:06
NODAL SOLUTION
STEP=1
SUB =1
TIME=1
TEMP (AVG)
RSYS=0
PowerGraphics
EFACET=1
AVRES=Mat
SMN =338.196
SMX =578.177
338.196
364.86
391.525
418.19
444.854
471.519
498.183
524.848
551.513
578.177

205

FIGURE 3-6

TEMPERATURE DISTRIBUTION,
FUEL ASSEMBLIES
(NORMAL CONDITIONS OF TRANSPORT)

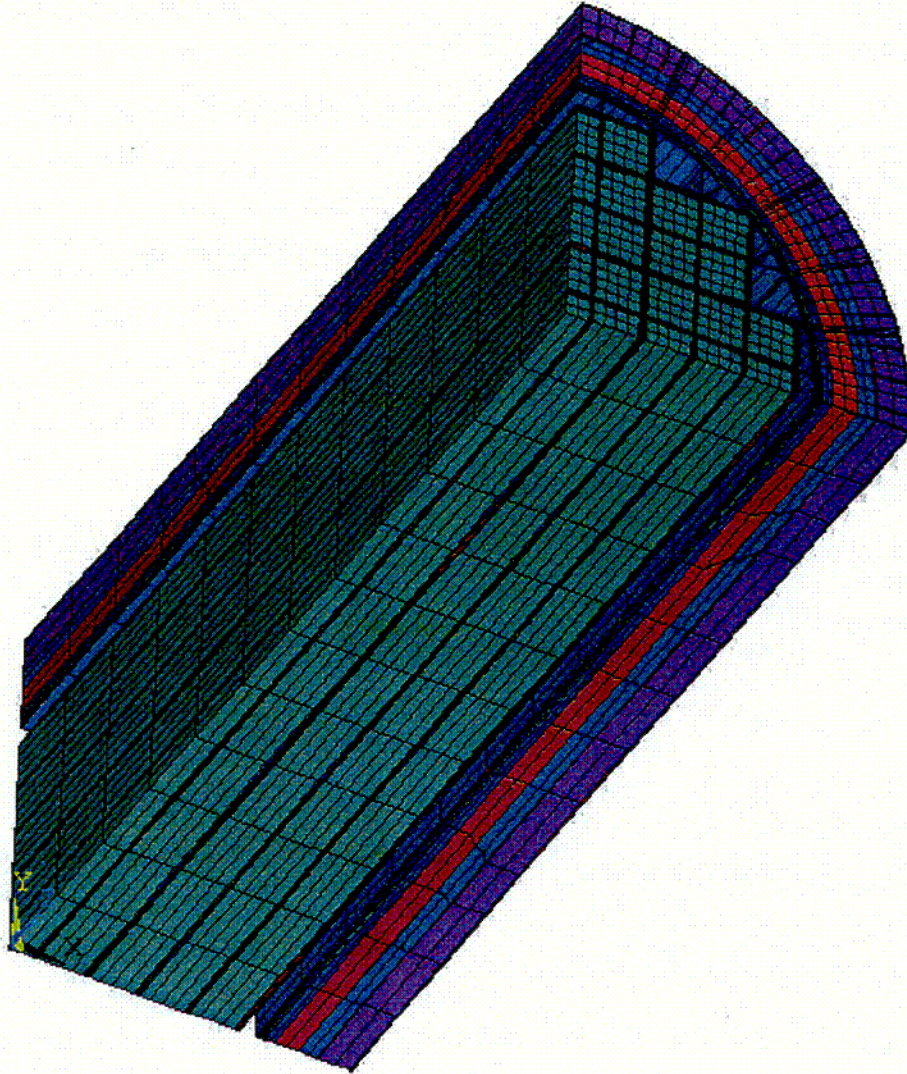


```
ANSYS 5.6
AUG 10 2000
07:41:33
NODAL SOLUTION
STEP=1
SUB =1
TIME=1
TEMP (AVG)
RSYS=0
PowerGraphics
EFACET=1
AVRES=Mat
SMN =356.875
SMX =597.995
356.875
383.666
410.457
437.248
464.039
490.83
517.621
544.413
571.204
597.995
```

CO6

FIGURE 3-7

FINITE ELEMENT PLOT,
CASK CROSS-SECTION MODEL

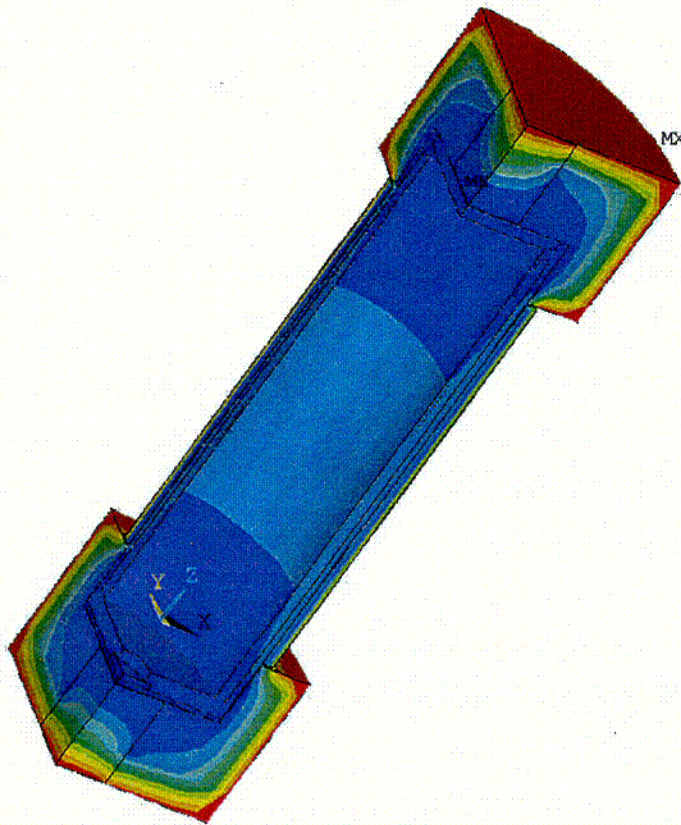


C07

Rev. 0 4/01

FIGURE 3-8

TEMPERATURE DISTRIBUTION,
CASK BODY MODEL, END OF FIRE
(HYPOTHETICAL ACCIDENT CONDITIONS)

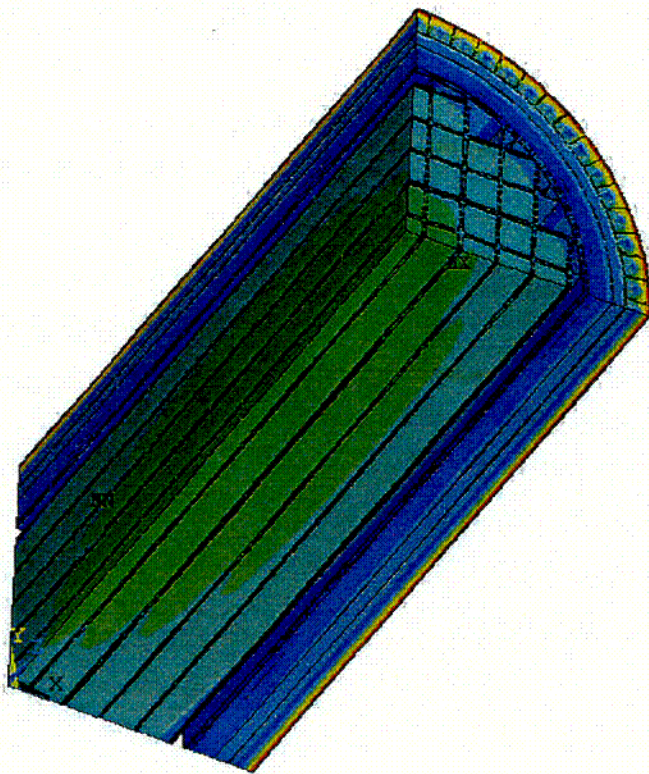


ANSYS 5.6
NOV 7 2000
10:41:03
NODAL SOLUTION
STEP=2
SUB =9
TIME=.5
TEMP (AVG)
RSYS=0
PowerGraphics
EFACET=1
AVRES=Mat
SMN =195.933
SMX =1456
195.933
335.981
476.029
616.076
756.124
896.172
1036
1176
1316
1456

C08

FIGURE 3-9

TEMPERATURE DISTRIBUTION,
CASK CROSS SECTION MODEL, END OF FIRE
(HYPOTHETICAL ACCIDENT CONDITIONS)

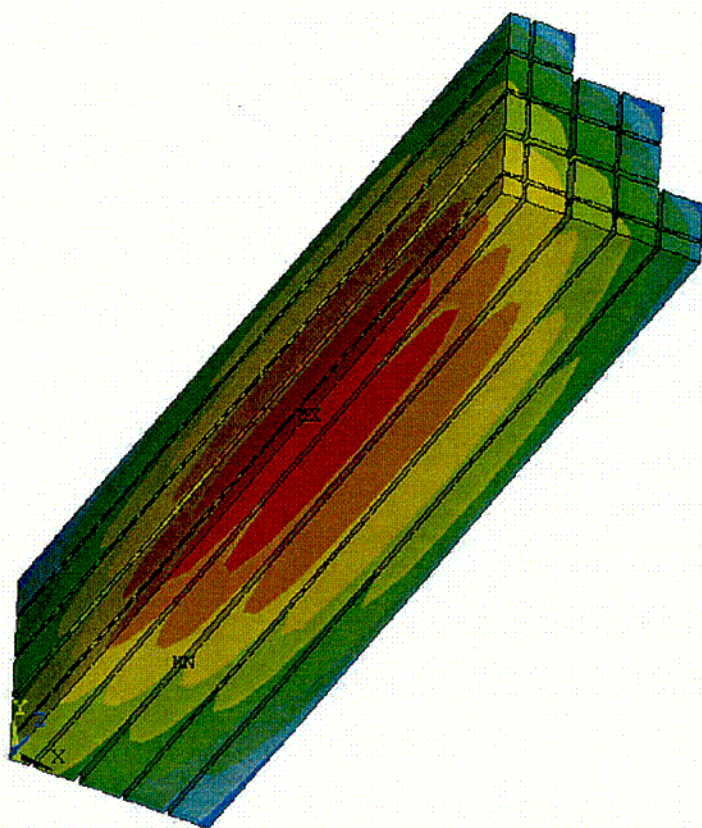


ANSYS 5.6
SEP 19 2000
07:38:34
NODAL SOLUTION
STEP=2
SUB =7
TIME=.5
TEMP (AVG)
RSYS=0
PowerGraphics
EFACET=1
AVRES=Mat
SMN =287.093
SMX =1103
287.093
377.697
468.302
558.907
649.511
740.116
830.72
921.325
1012
1103

C09

FIGURE 3-10

TEMPERATURE DISTRIBUTION,
FUEL ASSEMBLIES, PEAK TEMPERATURES
(HYPOTHETICAL ACCIDENT CONDITIONS)

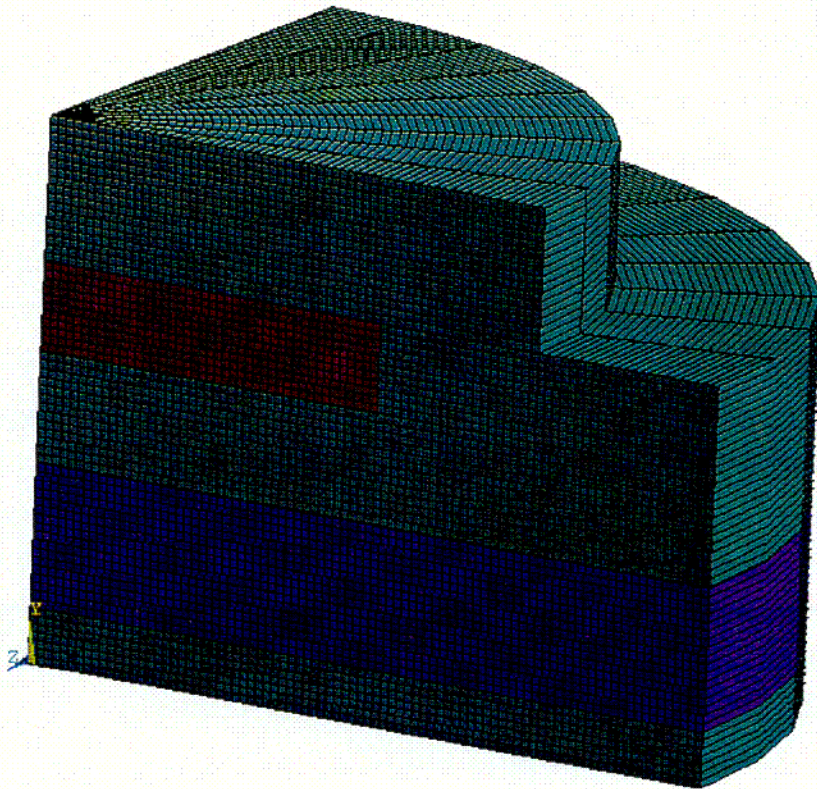


ANSYS 5.6
SEP 19 2000
07:40:17
NODAL SOLUTION
STEP=3
SUB =20
TIME=27.856
TEMP (AVG)
RSYS=0
PowerGraphics
EFACET=1
AVRES=Mat
SMN =469.902
SMX =680.448
469.902
493.296
516.69
540.084
563.478
586.872
610.266
633.66
657.054
680.448

C10

FIGURE 3-11

FINITE ELEMENT PLOT,
TRUNNION REGION MODEL



C11

Rev. 0 4/01

FIGURE 3-12

TEMPERATURE DISTRIBUTION,
TRUNNION REGION MODEL
(TIME = 4.7 HOURS)

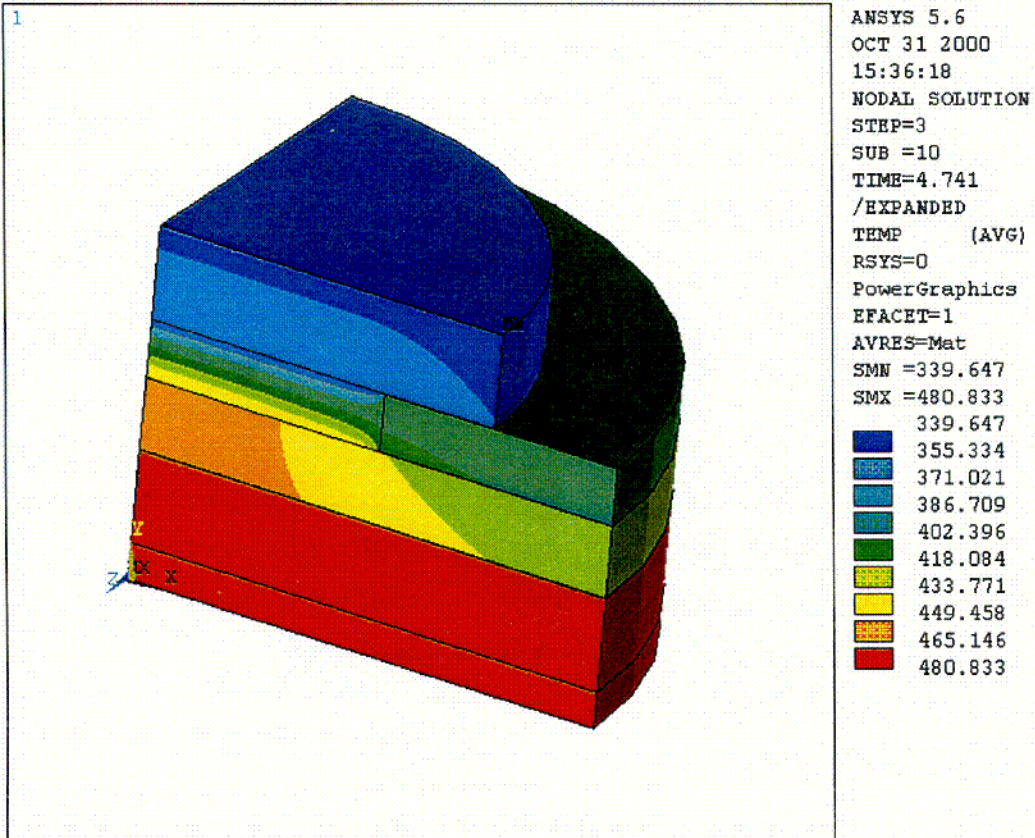
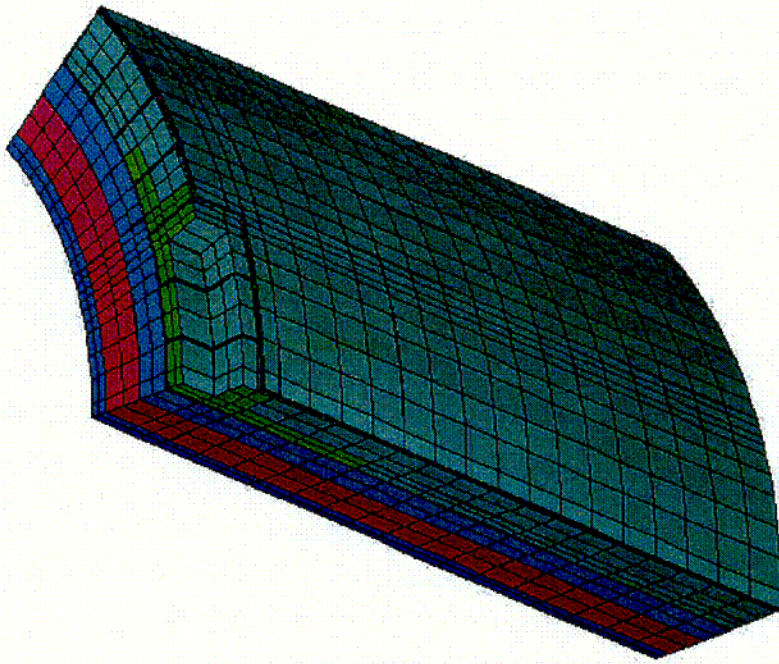


FIGURE 3-13

FINITE ELEMENT PLOT,
BEARING BLOCK REGION MODEL

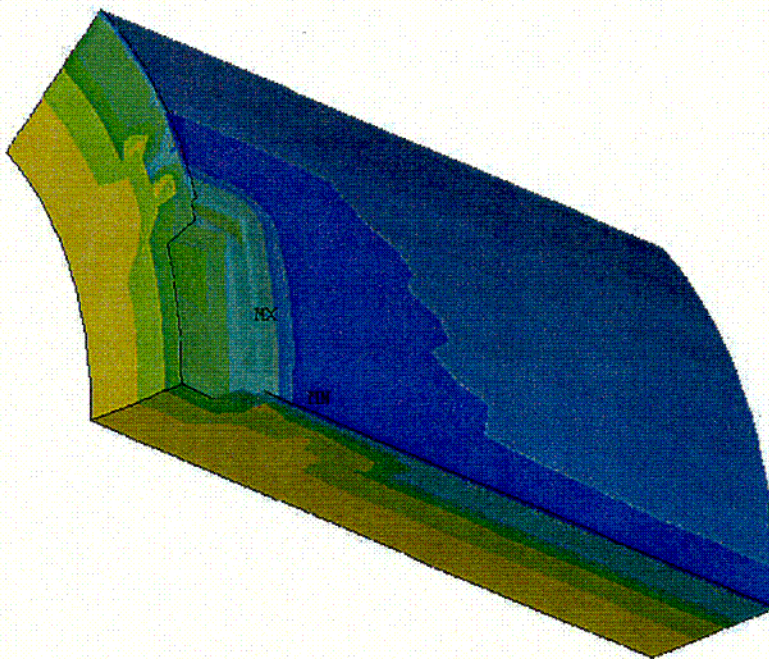


C13

Rev. 0 4/01

FIGURE 3-14

TEMPERATURE DISTRIBUTION,
BEARING BLOCK REGION MODEL
(TIME = 2.9 HOURS)



```
ANSYS 5.6  
DEC 1 2000  
10:31:28  
NODAL SOLUTION  
STEP=3  
SUB =10  
TIME=2.85  
TEMP  
SMN =309.574  
SMX =485.176  
309.574  
329.085  
348.596  
368.108  
387.619  
407.13  
426.642  
446.153  
465.664  
485.176
```

C14